

# Excitation-Neurogenesis Coupling in Adult Neural Stem/Progenitor Cells

Karl Deisseroth,<sup>1,3,\*</sup> Sheela Singla,<sup>1,3</sup>  
Hiroki Toda,<sup>2</sup> Michelle Monje,<sup>2</sup>  
Theo D. Palmer,<sup>2</sup> and Robert C. Malenka<sup>1,\*</sup>

<sup>1</sup>Nancy Pritzker Laboratory  
Department of Psychiatry and Behavioral Sciences

<sup>2</sup>Department of Neurosurgery  
Stanford University School of Medicine  
Stanford, California 94305

## Summary

A wide variety of *in vivo* manipulations influence neurogenesis in the adult hippocampus. It is not known, however, if adult neural stem/progenitor cells (NPCs) can intrinsically sense excitatory neural activity and thereby implement a direct coupling between excitation and neurogenesis. Moreover, the theoretical significance of activity-dependent neurogenesis in hippocampal-type memory processing networks has not been explored. Here we demonstrate that excitatory stimuli act directly on adult hippocampal NPCs to favor neuron production. The excitation is sensed via Ca<sub>v</sub>1.2/1.3 (L-type) Ca<sup>2+</sup> channels and NMDA receptors on the proliferating precursors. Excitation through this pathway acts to inhibit expression of the glial fate genes *Hes1* and *Id2* and increase expression of *NeuroD*, a positive regulator of neuronal differentiation. These activity-sensing properties of the adult NPCs, when applied as an “excitation-neurogenesis coupling rule” within a Hebbian neural network, predict significant advantages for both the temporary storage and the clearance of memories.

## Introduction

In the adult mammalian hippocampus, production of new neurons is influenced by a variety of environmental and behavioral conditions (Brown et al., 2003; McEwen, 1994; Arvidsson et al., 2001; Cameron and McKay, 1998; Taupin and Gage, 2002; Santarelli et al., 2003). These findings have stimulated great interest in determining if hippocampal activity itself meaningfully guides neurogenesis, thereby implementing a novel form of network plasticity at the cellular level that would go beyond the well-known forms of plasticity that occur at the synaptic level (Malenka and Nicoll, 1999; Kandel, 2001; Sejnowski, 1999). In adult songbirds, regulation of neurogenesis is tightly linked to the behavioral demands associated with song generation (Alvarez-Buylla et al., 1990; Nottebohm, 2002; Louissant et al., 2002). Likewise in mammals, the insertion of new neurons could modulate the capability of the adult hippocampal network to handle the storage of new memories or the clearance of old memories (Feng et al., 2001; Shors et al., 2001). Further-

more, linking neurogenesis to neuronal activity could adapt the adult network both to physiological demands and to pathological insults (Alvarez-Buylla et al., 2002; Bjorklund and Lindvall, 2000; Cameron and McKay, 1998; Gould et al., 2000; Malberg et al., 2000; Parent et al., 1997; Park et al., 2002; Seaberg and van der Kooy, 2002; Snyder et al., 1997; Taupin and Gage, 2002; Temple, 2001; Watt and Hogan, 2000; Santarelli et al., 2003).

Many interventions that likely modulate hippocampal neuronal activity levels affect adult neurogenesis (Cameron et al., 1995; Gould et al., 2000; Madsen et al., 2000; Malberg et al., 2000; Parent et al., 1997). For example, brief NMDA receptor blockade *in vivo* increases precursor proliferation and subsequent neuron production (Cameron et al., 1995; Gould et al., 2000). However, it is not known if this excitatory glutamate receptor blockade translates into stably decreased hippocampal activity. In fact, other global interventions, which would be expected to *increase* activity (e.g., running, status epilepticus, enriched environments) (Madsen et al., 2000; Malberg et al., 2000; Parent et al., 1997; van Praag et al., 1999), paradoxically also increase proliferation and subsequent neuron production. Central to this paradox is the possibility that, in some experimental conditions, activity is directly sensed by the proliferating progenitor cells themselves, while in others, activating stimuli instead have indirect effects on the proliferating progenitors, for example, via induced release of local growth factors (Kokaia and Lindvall, 2003).

Using an array of *in vitro* and *in vivo* approaches, we have addressed this issue, focusing on four specific questions: (1) under controlled conditions, what is the actual relationship between excitation and adult neurogenesis (if any)? (2) are proliferating adult progenitor cells themselves computational elements capable of responding to local activity signals? (3) how are these signals transduced to influence the production of new neurons? and (4) what are the computational advantages of coupling excitation to neurogenesis for the functioning of mature brain networks?

## Results

### In Vitro System for Studying the Relationship of Excitation to Neurogenesis

As noted above, *in vivo* manipulations that are thought to influence hippocampal activity affect proliferation and survival of adult neural stem/progenitor cells (NPCs), but the results do not fit into an easily reconcilable pattern (reviewed in Gould et al., 2000). Although these *in vivo* approaches are clearly important, it is difficult to precisely control and measure activity levels *in vivo* in a rigorous fashion. Furthermore, it is difficult *in vivo* to determine which cell type(s) directly senses any changes in activity, much less elucidate the detailed molecular mechanisms that are responsible. Therefore, to directly determine the neurogenic effects of activity on proliferating adult NPCs (excitation-neurogenesis coupling), it was necessary to begin with a reduced

\*Correspondence: malenka@stanford.edu (R.C.M.); deissero@stanford.edu (K.D.)

<sup>3</sup>These authors contributed equally to this work.

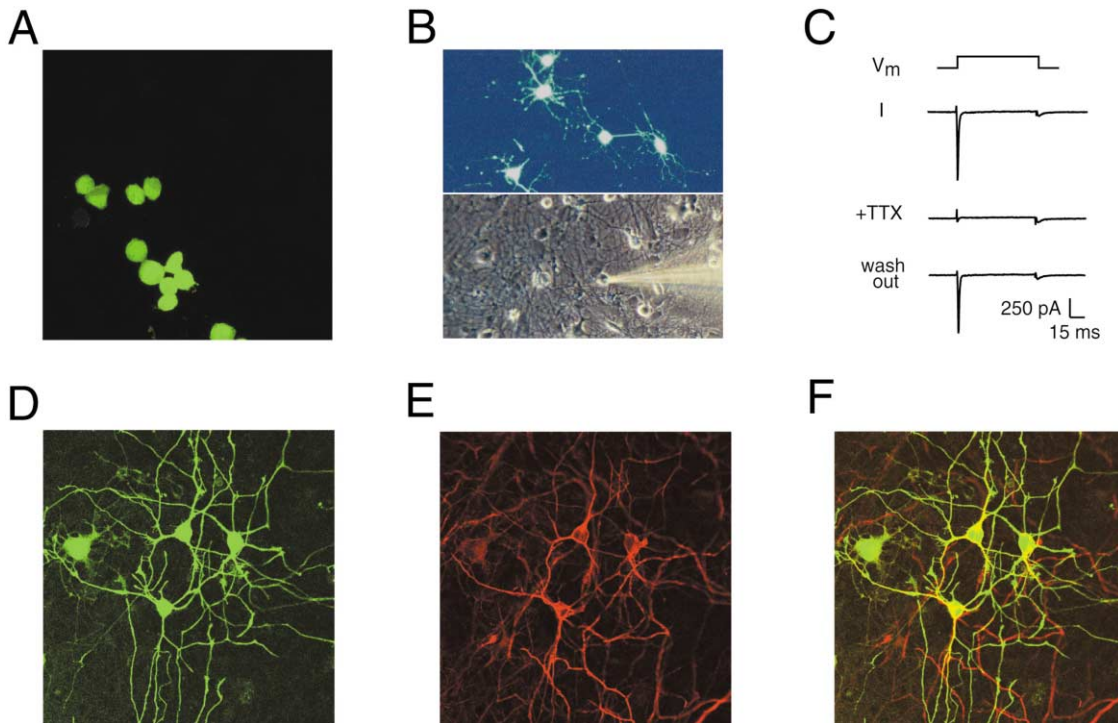


Figure 1. In Vitro System for Studying the Effects of Excitation on Neurogenesis

(A) GFP-labeled adult hippocampal HC37 NPCs in proliferative culture.

(B) Whole-cell patch-clamp recording from a differentiated NPC-derived neuron in coculture. HC37 cells were grown with hippocampal neurons and glia in retinoic acid-containing medium permitting neuronal differentiation.

(C) Example of voltage-activated Na<sup>+</sup> current evoked from an NPC-derived neuron. Tetrodotoxin (TTX, 1  $\mu$ M) reversibly blocked the inward current evoked with a step from  $-70$  mV to  $-10$  mV.

(D) Morphology of differentiated NPC progeny: GFP expression shown.

(E) Same field of cells as in (D); MAP2ab expression shown. Cells lacking neuronal morphology (cell on the left without two to five well-defined primary processes) consistently expressed little MAP2ab, while cells with neuronal morphology (three cells on the right) expressed high levels of MAP2ab.

(F) Overlay of GFP (green) and MAP2ab (red) expression. Here and in subsequent figures, overlap of expression is indicated in yellow.

in vitro system to provide uniform proliferative conditions, defined excitation and differentiation stimuli, and full physiological characterization of the resulting differentiated cells.

To examine stem/progenitor cell behavior in the presence of mature neurons and glia, we employed green fluorescent protein (GFP)-labeled adult rat hippocampal NPCs (Palmer et al., 1997). There is active debate over the precise lineage potential and heterogeneity of adult hippocampal NPCs in vivo, and the field currently lacks validated markers for early stages of lineage restriction. Therefore, to model this native cell population, we used well-characterized cultures of proliferating cells isolated directly from adult rat hippocampus (Figure 1A). These cells have been shown to retain stem cell phenotypes in vitro (Palmer et al., 1997) and behave identically to endogenous NPCs when implanted into the intact hippocampus, participating normally in hippocampal neurogenesis (Monje et al., 2002; Palmer et al., 1997).

The fraction of neurons produced from proliferating precursors is substantial at baseline ( $\sim 50\%$ – $80\%$ ) in the hippocampus of behaving adult rodents. We therefore used baseline in vitro conditions that favor neuronal differentiation. Using established techniques, we plated the proliferating NPCs (Figure 1A) onto primary hippo-

campal cultures (Song et al., 2002) followed by mitogen taper in medium that permits neuronal differentiation (see Experimental Procedures). After 14 days,  $\sim 24\%$  of the cells had differentiated into neurons, expressing the neuronal somatodendritic protein MAP2ab. Neuronal tetrodotoxin (TTX)-sensitive voltage-gated Na<sup>+</sup> currents were also expressed, as determined by whole-cell patch clamp (Figures 1B and 1C). Validating the use of MAP2ab as a neuronal marker, the cells that displayed typical mature neuronal morphology (two to five well-defined primary processes; Claiborne et al., 1990) consistently expressed far greater MAP2ab expression than other cells ( $3.86 \pm 0.28$ -fold increased MAP2ab intensity measured in confocal sections; illustrated in Figures 1D–1F).

#### Excitation Promotes Neurogenesis from Adult NPCs

We next investigated the impact of excitation on neurogenesis by applying modest depolarizing levels of extracellular potassium (20 mM) synchronously with the initiation of mitogen taper (termed day 1). This manipulation mimics the effects of stably increased activity as would occur in an active neural network. We observed an increase in neuron production under these conditions (measured by MAP2ab staining as in Figure 1) compared

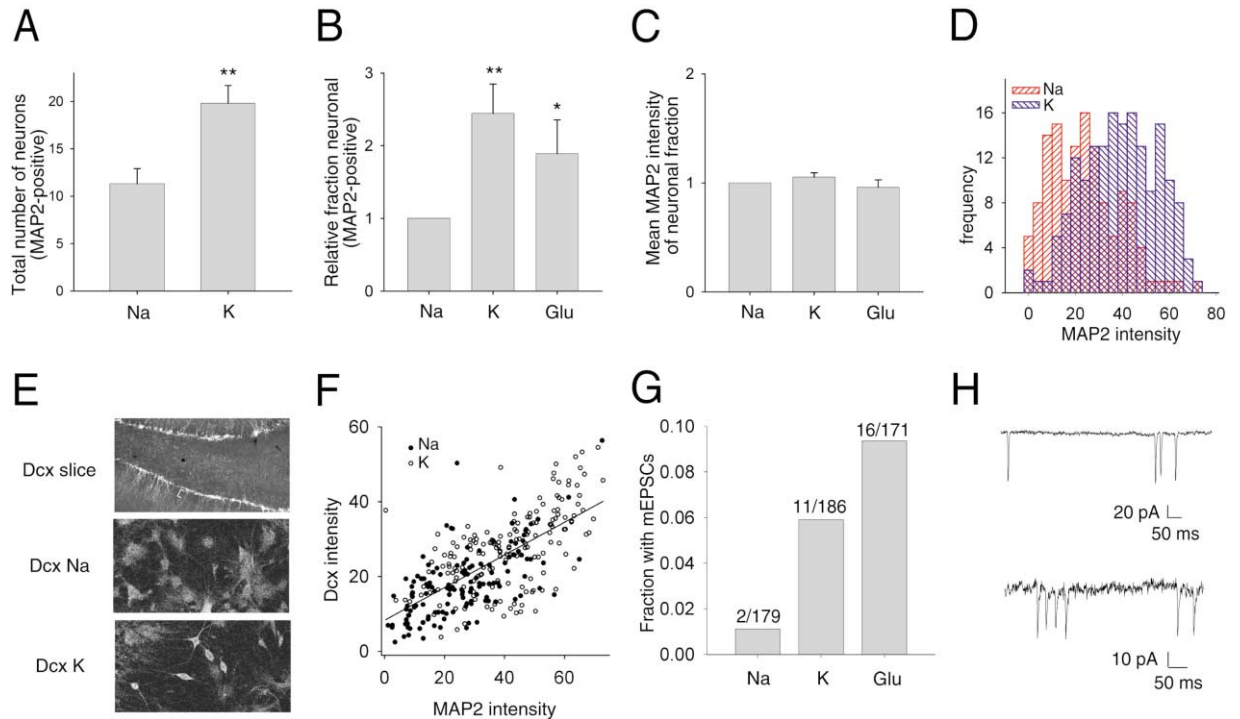


Figure 2. Excitation Promotes Neurogenesis from Adult NPCs

(A) Depolarization (K) elevated the total neuron number in ten randomly selected 40× microscope fields by comparison with control (Na) conditions (n = 12 independent experiments; \*p < 0.05; \*\*p < 0.01 here and in subsequent figures).  
 (B) Depolarization (K) (n = 12 independent experiments) or glutamate application (Glu; n = 6 independent experiments) elevated the fraction of neurons among the NPC progeny. The fraction of GFP+ cells that were MAP2ab+ is normalized to the fraction found in the Na condition. Mean neuronal fraction in this control condition across all experiments was 24%.  
 (C) There was no effect of either stimulus on the mean MAP2ab intensity in the resulting neuronal progeny (p = 0.21 for K; p = 0.40 for Glu) or in the nonneuronal progeny (data not shown).  
 (D) MAP2ab intensity versus frequency histogram of cells in control (Na) or depolarized (K) conditions from a representative experiment. Depolarization increased the proportion of cells expressing high levels of MAP2ab without generating cells that expressed MAP2ab at levels higher than those observed in control conditions.  
 (E) (Top) Doublecortin (Dcx) staining in adult rat dentate gyrus; young neurons still lining the subgranular zone and sending processes into the granule cell layer (bracket) express this early marker. Dcx staining in vitro, in the control (Na; middle panel) and excitation (K; bottom panel) conditions.  
 (F) Graph shows correlation between excitation-induced increases in MAP2ab and Dcx at the single-cell level (n = 304; r<sup>2</sup> = 0.4654; p < 0.0001).  
 (G) Excitation increased the fraction of cells with functional excitatory synapses as defined by the occurrence of miniature EPSCs.  
 (H) Sample mEPSCs from the control (Na; upper trace) and glutamate (lower trace) conditions.

to the nondepolarizing control condition in which equivalent sodium was added as an osmotic control (Figure 2A).

This increased neuron production was not due to a nonspecific increase in the number of all cells; rather, it was due to an increase in the fraction of the NPCs that became neurons (Figure 2B). Direct application of the excitatory neurotransmitter glutamate also gave rise to an increase in the fraction of NPCs becoming neurons (Figure 2B), indicating that the increased neurogenesis was independent of the method of excitation. This effect was not simply on the rate or extent of differentiation, as (1) mean MAP2ab intensity values in the resulting neuronal progeny were not higher in the excitation condition (Figure 2C), (2) no new higher-MAP2ab value histogram bins resulted from stimulation when compared to control conditions (Figure 2D), (3) cells scored as nonneuronal NPC progeny also did not exhibit any difference in MAP2ab expression between the different experimental conditions, maintaining a consistently low

level of background staining (data not shown), and (4) in neuronal progeny with TTX-sensitive sodium channel currents, current density was not altered by depolarization (data not shown). Moreover, excitation did not affect adult NPC progeny proliferation, survival, or apoptosis under these conditions (see Figure 6), indicating that excitation favors adoption of the neuronal phenotype (Figures 2B and 2D).

Additional measures confirmed the finding that excitation increased the fraction of adult NPCs that became neurons. Expression of the neuron-specific protein Dcx (Figure 2E) (Nacher et al., 2001), which is structurally and functionally distinct from MAP2ab, was increased by the depolarization treatment and correlated with MAP2ab expression (Figures 2E and 2F). Furthermore, excitation with glutamate or depolarization caused an increase in the fraction of adult NPCs that received functional excitatory synaptic connections, determined electrophysiologically with whole-cell patch-clamp recording (Figures 2G and 2H). This is a key functional

measure that indicates an increase in the fraction of cells adopting neuronal characteristics. We also tested whether the observed adult excitation-neurogenesis coupling was generalizable to other NPC preparations by examining an independently derived early-passage adult hippocampal NPC population (RH-1). Excitatory stimuli also promoted neurogenesis in this line, as evidenced by the increased proportion of cells with MAP2ab expression (data not shown). Thus, the results from several independent assays and examination of two independent cell lines indicate that excitatory stimuli favor the production of fully functional neurons from proliferating adult NPCs.

### Excitation Acts Directly on Adult Hippocampal NPCs

The preceding data address the central question of whether excitation increases or decreases neuron production from adult hippocampal NPCs and suggest that stably active neural networks could adaptively respond by inserting new neurons. However, a key mechanistic question is left unanswered. Is the impact of excitation directly on the NPCs (for example, on intrinsic ion channels) or indirectly on the surrounding mature hippocampal cells (for example, through depolarization-induced release of a growth factor)?

To answer this question, we employed an intervention not possible *in vivo*. Instead of the living hippocampal coculture environment, we used an ethanol-fixed and extensively washed hippocampal culture as substrate; this is a setting that maintains an environment permissive for neurogenesis (Song et al., 2002) but in which the *only* living cells are the adult NPCs. Under these conditions, we found that proliferating NPCs themselves responded to excitatory stimuli (depolarization or glutamate) with elevations in intracellular  $Ca^{2+}$  (measured with the visible  $Ca^{2+}$ -sensitive dye X-rhod-1; Figures 3A and 3B), indicating expression of responsive  $Ca^{2+}$  signaling within the proliferating NPC population. 44 of 73 cells showed an increase with glutamate, and 39 of 50 with depolarization; the actual number of responders is likely higher, as it is known that small juxtamembranous  $Ca^{2+}$  elevations on the submicron scale (not detectable by imaging) couple robustly to intracellular signaling processes (Deisseroth et al., 1998). If this intrinsic  $Ca^{2+}$  channel signaling contributes to neurogenesis, then stimulation of these cells grown on the fixed coculture substrate should still enhance neurogenesis. Indeed, we found that both the total number of new neurons (Figure 3C) and the fraction of MAP2ab-positive cells (Figure 3D; black bars) were enhanced by depolarization, just as in the living coculture condition. Functional synaptic connectivity between the cells themselves was also enhanced, evidenced by the increased occurrence of spontaneous synaptic currents (Figure 3F). As the only living cells in the cultures are the NPCs, these data formally demonstrate that excitation acts directly on the NPCs to promote neurogenesis.

How exactly does the excitation influence the NPCs? Excitation by depolarization could act through voltage-activated  $Ca^{2+}$  ( $Ca_v$ ) channels, which play a variety of roles in mediating neuronal responses. While  $Ca_v2.1$  (N-type) and  $Ca_v2.2$  (P/Q-type)  $Ca^{2+}$  channels play criti-

cal roles in neuronal synaptic transmission,  $Ca_v1.2/1.3$  (L-type)  $Ca^{2+}$  channels have been implicated in neuronal synaptic plasticity and survival (West et al., 2001) and play a unique and privileged role among the various voltage-sensitive  $Ca^{2+}$  channel types in membrane-to-nucleus signaling that modulates activity-dependent gene expression programs (Deisseroth et al., 1998). It is not known, however, which (if any) of these channel types could be involved in adult excitation-neurogenesis coupling. We explored this issue by employing potent and selective antagonists in the fixed-substrate environment. We found that the peptide  $Ca_v2.1/2.2$  channel antagonist  $\omega$ -Ctx-MVIIC did not inhibit neurogenesis (data not shown), while the dihydropyridine  $Ca_v1.2/1.3$  channel antagonist nifedipine completely blocked excitation-induced neurogenesis (Figure 3D; light gray bars). We next made use of the  $Ca_v1.2/1.3$  channel agonist FPL 64176 as the only external stimulus and conversely observed an enhancement of neurogenesis (Figure 3D; dark gray bars), demonstrating that  $Ca_v1.2/1.3$  channel activation on NPCs is sufficient to promote their neurogenesis.

Certain functions of  $Ca_v1.2/1.3$  channels can also be served by NMDA receptors; the two channel types often provide overlapping effects, likely due to a common ability to recruit calmodulin signaling (Deisseroth et al., 1998). NMDA receptors have been implicated in synaptic plasticity (Bear and Malenka, 1994; Malenka and Nicoll, 1999), gene expression (West et al., 2001), and memory formation (Bear and Malenka, 1994), and play a role in dentate gyrus cell proliferation (Arvidsson et al., 2001; Cameron et al., 1995; Gould et al., 2000; Liu et al., 1998). However, the sign and magnitude of effects of NMDA receptor antagonists on progenitor cells *in vivo* have differed qualitatively, depending on the experimental paradigm (Arvidsson et al., 2001; Cameron et al., 1995; Gould et al., 2000; Liu et al., 1998). To test the contribution of NMDA receptors to excitation-neurogenesis coupling under controlled conditions *in vitro*, we applied the specific NMDA receptor antagonist D-AP5, which inhibited both basal neurogenesis and the enhanced neurogenesis elicited by  $K^+$  treatment. Conversely, the specific NMDA receptor agonist NMDA elicited a significant increase in neurogenesis (Figure 3E).

These experiments, in an environment where no other living cells are present, demonstrate that multiple activity-sensing  $Ca^{2+}$  influx pathways are present and functioning on adult NPCs and that activation of these pathways promotes neurogenesis. Furthermore, this effect does not depend on indirect activity-dependent signals acting via mature neurons or glia. Therefore, NPCs themselves can act as the signal detection and processing elements mediating adult excitation-neurogenesis coupling.

### Immediate Impact of Excitation on Proliferating NPCs

By design, excitation stimuli were applied to the proliferative NPCs concurrently with conditions permitting differentiation, to mimic the hypothesized *in vivo* situation in which proliferating progenitors are exposed to network activity and exit the cell cycle. We next explored possible mechanisms by which the excitatory stimuli

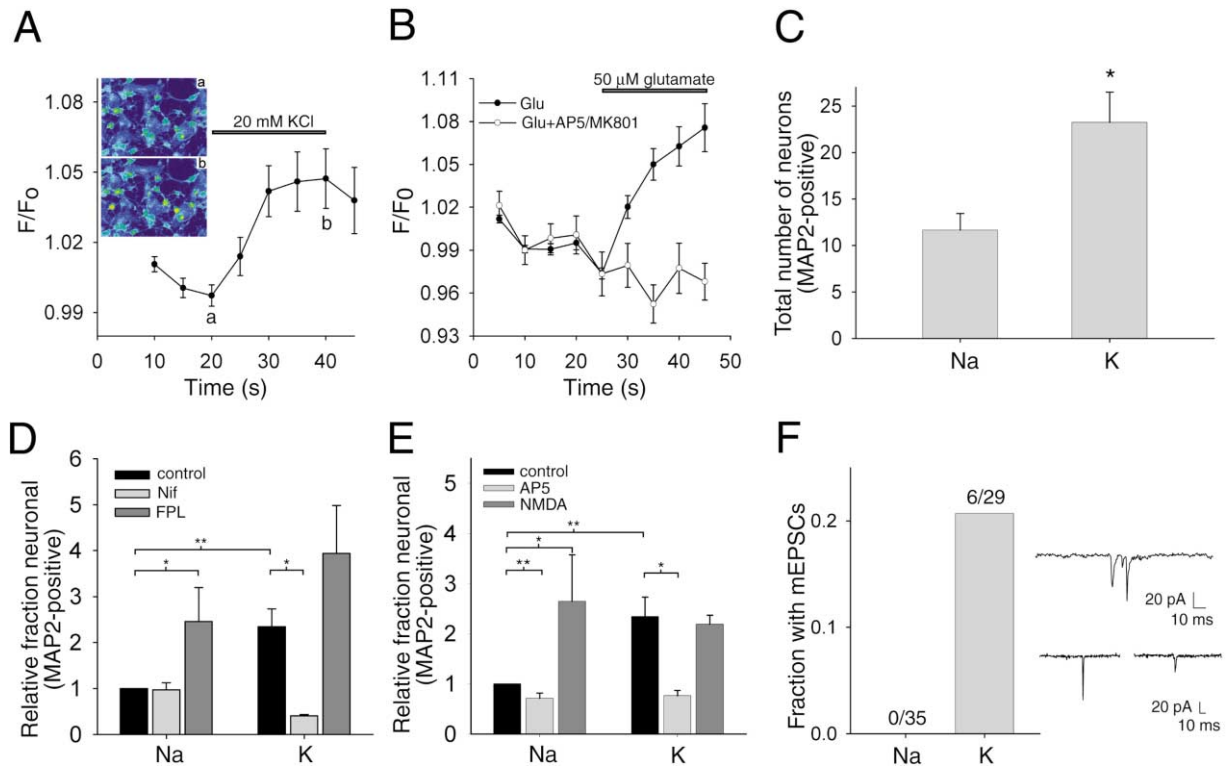


**Figure 3. Excitation Acts Directly on Adult Hippocampal NPCs**

(A) Depolarization with KCl causes elevations of  $[Ca^{2+}]_i$  in proliferating adult-derived NPCs grown on a fixed substrate of hippocampal cultures. Graph shows x-Rhod-1 fluorescence expressed as  $F/F_0$ ; increased fluorescence indicates elevated  $[Ca^{2+}]_i$ , which is superimposed on slow photobleaching of the indicator. Mean values of all loaded cells are shown ( $n = 50$  cells). Insets show pseudocolor images of the field of cells at time points corresponding to a and b. Warmer (longer wavelength) colors correspond to higher levels of  $[Ca^{2+}]_i$ .  
 (B)  $[Ca^{2+}]_i$  response to applied glutamate measured with x-Rhod-1 ( $n = 73$ ); response is blocked by the NMDA receptor antagonists 50  $\mu$ M AP5/10  $\mu$ M MK-801 ( $n = 17$ ).  
 (C) As in the living coculture condition, total neuron number in ten randomly selected fields was increased by excitation ( $n = 9$ ).  
 (D) Adult-derived NPCs cultured on a fixed hippocampal substrate display robust excitation-neurogenesis coupling ( $n = 7$  independent experiments). Bidirectional changes in neurogenesis result from application of  $Ca_v1.2/1.3$  channel agonist (FPL64176, 5  $\mu$ M) or antagonist (nifedipine, 10  $\mu$ M).  
 (E) Bidirectional changes in neurogenesis also result from application of NMDA receptor agonist (NMDA, 50  $\mu$ M) or antagonist (D-AP5, 50  $\mu$ M).  
 (F) Excitation enhances frequency of synaptic connectivity between NPCs plated on the fixed hippocampal substrate or with conditioned medium from hippocampal cells (light fixation: 0/23 Na, 4/17 K; hippocampal conditioned medium: 0/12 Na, 2/12 K). Traces on the right show sample mEPSCs.

might act, considering first whether excitation acts immediately (on the proliferating progenitors) or in a delayed fashion (for example, on cells that have exited the cell cycle and have started to differentiate into neurons).

To determine whether the excitatory stimuli were sensed by proliferative or postmitotic cells, the cells were labeled with BrdU for 24 hr beginning 1 day after plating on fixed substrate (starting at the time when excitatory stimuli are applied), then fixed and evaluated for BrdU incorporation. Nearly the entire population (>90%) of NPCs plated on the fixed substrate were rapidly proliferating and labeled with BrdU within this period, when excitatory stimuli are applied (Figure 4A). We found virtually no neuronal MAP2ab staining at this time point (data not shown). Moreover, it is these rapidly proliferating NPCs that respond to excitatory stimuli with increased neurogenesis, since even a single brief 5 min stimulus pulse applied at the beginning of this 24 hr BrdU labeling period (during which >90% of the cells are rapidly dividing) elicited significant excitation-neuro-

genesis coupling (Figure 4B). Conversely, all neurogenic effects were abolished when the antimetabolic agent FUdR was added at this time; under these conditions, more than 95% of all cells were killed, confirming the high mitotic index within cells responding to even brief excitation stimuli (data not shown). These results demonstrate that brief excitation applied to actively proliferating NPCs is sufficient for excitation-neurogenesis coupling. We also found that 5 min spaced pulses of depolarization or the  $Ca_v1.2/1.3$  channel agonist FPL 64176 on days 1, 3, and 5 enhanced neurogenesis to a similar extent as continuous excitatory stimulation (Figure 4B), indicating that even brief bouts of excitation are sufficient to strongly drive excitation-neurogenesis coupling via activity-sensitive  $Ca^{2+}$  channels within the proliferative NPC population.

The long-lasting effects of brief stimuli indicated that excitation might lead to alterations in transcriptional activities in dividing cells that could modulate stable changes in progeny phenotype. To begin to characterize

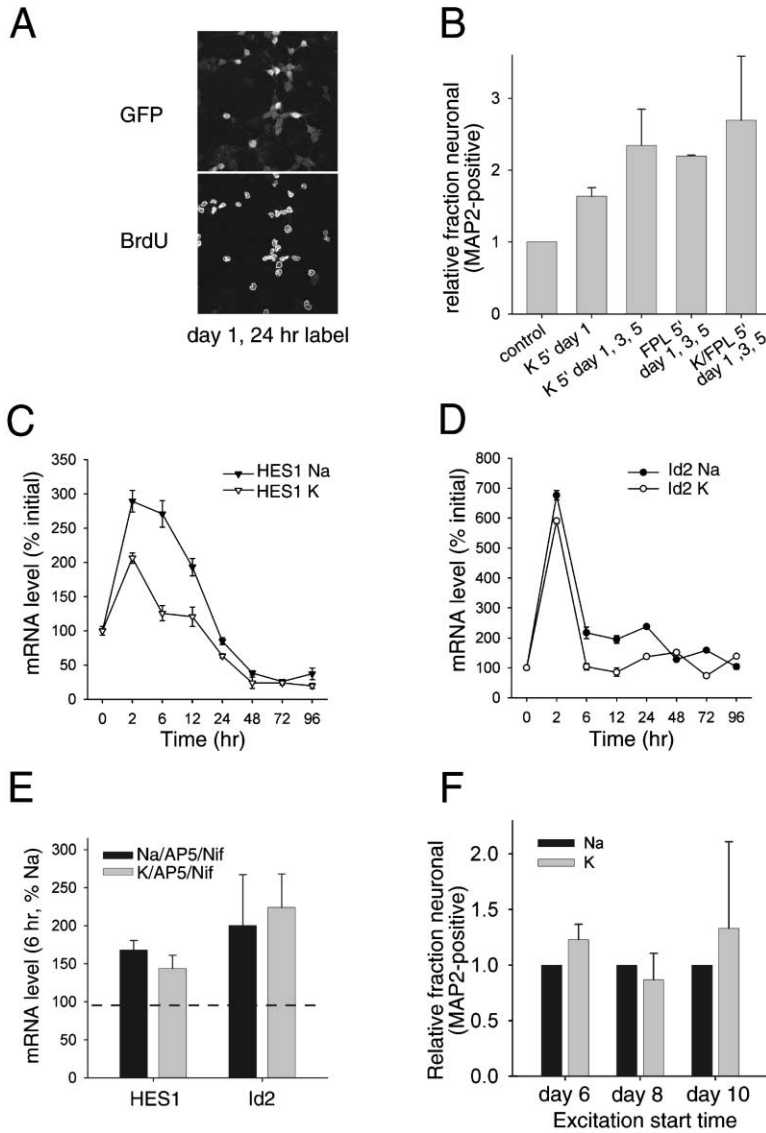


Figure 4. Immediate Impact of Excitation on Proliferating NPCs

(A) More than 90% of the NPCs were BrdU+ after a 24 hr label beginning on day 1 when excitation stimuli are applied.

(B) A single 5 min depolarizing pulse to the proliferating cells on day 1 was sufficient for significant excitation-neurogenesis coupling ( $n = 5$ ;  $p < 0.05$ ). Three 5 min pulses spaced every other day (day 1, 3, and 5 after substrate plating) were also effective when given as depolarization (K), direct Ca<sub>v</sub>1.2/1.3 channel activation with FPL 64176 (FPL), or the combination (K/FPL).

(C) Real-time PCR analysis of gene expression: *Hes1*. Proliferating NPCs were stimulated at the usual time (day 1 after plating on fixed substrate in mitogens) along with medium permissive of neuronal differentiation, and excitation (K) was supplemented with FPL 64176 as in Figure 3. Transcript level values were normalized to GAPDH transcript levels, and values shown are percent of initial ( $t = 0$ ) values. Each sample was tested in five replicates, and similar results were observed in three independent experiments.

(D) *Id2* likewise was inhibited by excitation, although first effects were not clearly apparent until 6 hr.

(E) Level of bHLH gene expression at the 6 hr time point in the presence of Ca<sup>2+</sup> channel antagonists. Dashed line corresponds to the unstimulated (Na)/no drug condition for each gene. AP5/nifedipine treatment drives gene expression in the opposite direction as excitation (compare this increase with the decrease in the antineuronal fate genes seen at 6 hr in [C] and [D]), and also blocks excitation-induced changes in the bHLH genes.

(F) Excitation applied to postmitotic cells does not give rise to excitation-neurogenesis coupling; depolarization was initiated on day 6, 8, or 10, and phenotype was assayed on day 14 ( $n = 3$ ;  $p > 0.2$  for all three conditions).

how proliferating NPCs respond to excitation, we explored the expression dynamics of transcription factors that influence cell phenotype by using real-time rtPCR, again in the fixed-substrate environment to ensure that any observed changes in gene expression must have occurred in the proliferating NPCs. We tracked the expression of the mammalian *hairy/Enhancer of split* homologs *HES1* and *HES5* (basic helix-loop-helix or bHLH genes that inhibit the neuronal phenotype in proliferating progenitors) (Jan and Jan, 1993; Tanigaki et al., 2001), the bHLH gene *Id2* (which also inhibits development of the neuronal phenotype) (Toma et al., 2000; Wang et al., 2001), and mammalian *acheate-scute homolog-1* (*MASH1*, a multifunctional bHLH gene that can modulate neuron production and is known to modulate *HES1/HES5* expression in proliferating progenitors) (Cai et al., 2000; Cau et al., 2000, 2002). Under the same conditions as those in Figure 3, we measured the transcript levels of these genes over the first 96 hr following differentiation under a range of conditions, including the presence or

absence of excitation and the presence or absence of channel blockers (Figures 4C–4E).

Excitation provoked a rapid transcriptional modulation of *HES1* and *Id2* when applied as usual to the proliferating NPCs at day 1, after the first 24 hr of substrate attachment (Figures 4C and 4D). Both of these antineuronal phenotype genes were depressed rapidly (over 2–6 hr) in the excited sample compared to controls, with a time course lasting ~24 hr (2–96 hr time points shown). Relatively little change was seen in *MASH1* and *HES5* (data not shown), and little difference was observed by 24 hr after initiation of the excitation in any genes, indicating that the response in these phenotype-determining genes occurs soon after the initiation of the excitatory stimulation and during the period where virtually all cells are still proliferating (Figure 4A).

We next examined the effects of applying antagonists of Ca<sub>v</sub>1.2/1.3 channels and NMDA receptors and found that conversely this caused a relative increase in the expression of these antineuronal phenotype genes (Fig-

ure 4E). Furthermore, these same antagonists abolished the changes in gene expression caused by excitation (Figure 4E). As with the  $\text{Ca}^{2+}$  imaging data, these results indicate that most of the proliferating precursors respond to depolarization, since substantial  $\text{Ca}^{2+}$  channel-dependent gene expression changes are seen in the population average. Therefore,  $\text{Ca}^{2+}$  influx through NMDA receptors and  $\text{Ca}_v1.2/1.3$  channels expressed on the proliferating NPCs rapidly couples to relevant downstream nuclear signaling pathways.

Finally, to determine if any residual neurogenic effects of excitation occur late (after cell cycle exit), we delayed application of excitatory stimuli until after the cells had exited the cell cycle under differentiating conditions. Depolarization in these postmitotic cells had no significant effect on the abundance of new neurons (Figure 4F). Similarly, delayed application of D-AP5 on day 5 did not prevent excitation-neurogenesis coupling ( $2.76 \pm 0.95$ -fold neurogenesis enhancement,  $n = 7$  independent experiments, versus  $2.22 \pm 0.25$ -fold enhancement in control,  $n = 5$  experiments;  $p > 0.5$ ). Taken together, these data demonstrate that the impact of excitation is immediate and induces a specific gene expression pattern in the proliferating NPCs.

#### Constitutive *Id2* Expression Prevents Excitation-Neurogenesis Coupling

If activity-dependent downregulation of a bHLH transcription factor is involved in increasing neurogenesis, then preventing this regulation should inhibit the excitation-neurogenesis coupling. We reasoned that manipulation of *Id2* would be likely to reveal mechanistic information since (1) *Id2* is a broadly acting dominant-negative regulator of many bHLH transcription factors, and (2) activity-dependent downregulation of *Id2* was one of the strongest effects we observed. We predicted that if excitation-coupled neurogenesis is dependent at least in part on *Id2* downregulation, then expression of *Id2* from a *constitutive* promoter would reduce the ability of the cell to effectively control *Id2* levels and should impair excitation-neurogenesis coupling. Indeed, in NPC progeny identified by cotransfected DsRed, the excitation-induced increase in neurogenesis (Figures 5A and 5B) was largely blocked by constitutive expression of *Id2* (Figures 5C and 5D). Basal neuron production, however, was not affected (Figure 5D). These results provide further support for a role of excitation in altering precursor cell fate via a conserved proneural bHLH network regulated by membrane depolarization.

#### Excitation Induces *NeuroD*, a Regulator of Neuronal Differentiation, in Proliferating NPCs

Although depolarization and  $\text{Ca}^{2+}$ -dependent intracellular signaling can in various contexts modulate cell death, proliferation, or survival (Mao et al., 1999), we found no significant effect of the mild depolarization used here on apoptosis or proliferation at any time point (using daily TUNEL and BrdU labeling throughout the experiment; two time points shown in Figures 6A and 6B). There was also no effect on survival of NPC progeny, as daily total cell counts from 20 random fields were not significantly different between the excitation and control conditions (data not shown). In both conditions

after mitogen withdrawal there was a similar brief period of residual proliferation followed by a reduction in cell number leaving  $\sim 60\%$ – $70\%$  of initial plating numbers. Neuronal fraction in these experiments, defined as before as the mean MAP2ab<sup>+</sup> fraction, revealed the expected significant increase in response to excitation (Figure 6B). These results demonstrate that excitation by depolarization increases neurogenesis without significantly changing the proliferative rate, proliferative fraction, survival, or death of the adult NPC progeny.

To further examine whether changes in proliferation or survival are necessary for the immediate proneural impact of excitation, we measured the expression of *NeuroD*. *NeuroD* is a downstream regulator of neuronal differentiation that controls expression of a range of genes required for mature neuronal functioning, including structural proteins and ion channels, and coordinates terminal differentiation in dentate gyrus granule cells (Schwab et al., 2000). Although a great number of bHLH genes interact in intricate and highly redundant ways to control cell fate (Cau et al., 2000), if the net transcriptional effect caused by excitation of proliferating NPCs is to rapidly favor commitment to the neuronal phenotype, we predicted that this commitment would be signaled by a relative increase in expression of *NeuroD* after excitation. Indeed, unlike the antineuronal fate bHLH genes, *NeuroD* expression was rapidly (within 2–6 hr) increased by excitation in the NPCs (Figure 6C). While excitation-induced decreases in *HES1* and *Id2* were transient (Figures 4C and 4D), the excitation-induced increase in *NeuroD* expression remained elevated for 96 hr, befitting a gene required for neuronal function (Figure 6C).

Consistent with the  $\text{Ca}^{2+}$  channel dependence of excitation-neurogenesis coupling, the *NeuroD* increase was blocked by the same  $\text{Ca}^{2+}$  channel antagonists (Figure 6D). Furthermore, this downstream gene expression response was not seen in NPCs grown in the absence of fixed hippocampal substrate, an environment incompatible with neurogenesis (Figure 6D; NPCs were plated onto polyornithine/laminin substrate as in Song et al., 2002, but otherwise treated identically). Together, these data demonstrate that, in proliferating adult NPCs, excitation induces a gene expression pattern consistent with neuronal differentiation. The rapidity of the gene expression response further demonstrates that no changes in proliferation or survival are necessary to observe the immediate proneural impact of excitation.

#### $\text{Ca}^{2+}$ Channels and Activity Influence Neurogenesis in Intact Systems

The use of an in vitro culture preparation with a fixed substrate permitted a rigorous demonstration of the direct effects of excitation on actively proliferating NPCs. It was important, however, to test whether excitatory stimuli could have the same effects on neurogenesis in more intact (albeit less well experimentally controlled) systems. Therefore, we next performed experiments using the living coculture model (as in Figure 2). In this setting, both direct depolarization with  $\text{K}^+$  and application of glutamate still gave rise to increased neurogenesis, which was blocked by the selective NMDA receptor antagonist D-AP5 (Figure 7A). Similarly, the selective

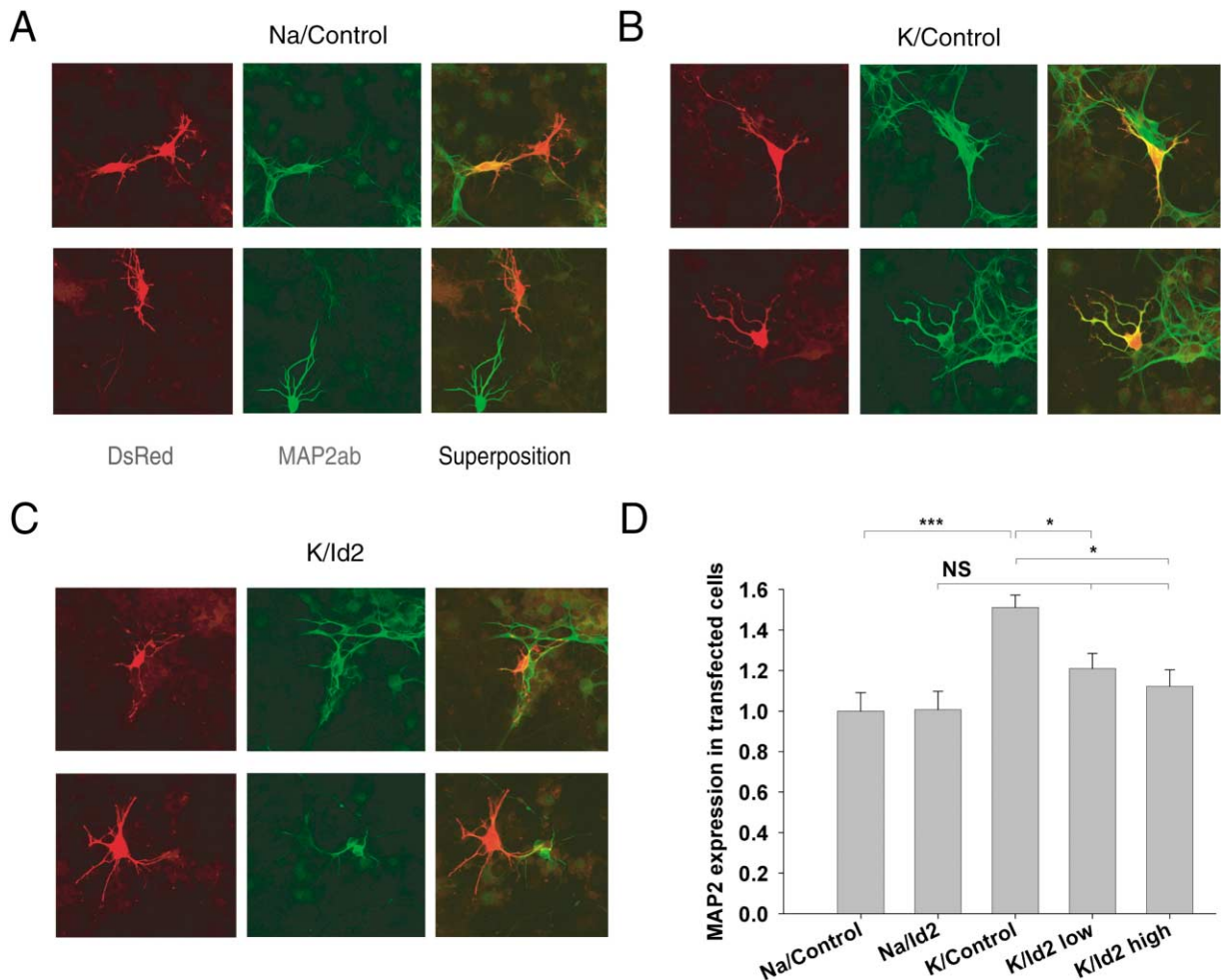


Figure 5. Constitutive *Id2* Expression Prevents Excitation-Neurogenesis Coupling

(A) Two representative fields of cells under basal excitation conditions (Na) and control plasmid transfection (Control). Left panels show DsRed cotransfection marker (red), middle panels show MAP2ab expression (green), and right panels show the superposition.  
 (B) Two representative fields of cells under stimulated excitation conditions (K) and control plasmid transfection (Control).  
 (C) Two representative fields of cells under excitation conditions (K) and constitutive *Id2* plasmid transfection (*Id2*).  
 (D) Summary graph showing that the increased neuronal phenotype expression associated with excitation in control transfections (Na/Control,  $n = 70$  cells versus K/Control,  $n = 75$  cells;  $***p < 0.001$ ) was largely blocked in the presence of constitutive *Id2*. Each condition was applied to three separate coverslips, and results of different doses of the *Id2* plasmid in two parallel experiments gave similar results (*Id2* low =  $0.4 \mu\text{g/well}$ , *Id2* high =  $1.8 \mu\text{g/well}$ ; K/Control versus K/*Id2* low,  $n = 46$  cells,  $p = 0.033$ ; K/Control versus K/*Id2* high,  $n = 36$  cells,  $p = 0.018$ ). The K/*Id2* conditions were not significantly different from Na/*Id2* (Na/*Id2* versus K/*Id2* low,  $p = 0.068$ ; Na/*Id2* versus K/*Id2* high,  $p = 0.228$ ). All values were normalized to the Na/Control condition. Basal neuron production was not affected by *Id2* (Na/Control versus Na/*Id2*,  $n = 87$  cells,  $p = 0.48$ ).

$\text{Ca}_v1.2/1.3 \text{ Ca}^{2+}$  channel antagonist nifedipine blocked depolarization-induced neurogenesis (Figure 7B). Both nifedipine and D-AP5 exhibited significant inhibition of neurogenesis in the basal (Na) condition as well (Figures 7A and 7B), suggesting some basal activation of these channels. Although multiple countervailing influences could come into play in the presence of living neurons and glia, these results are consistent with our previous observations that excitation promotes neurogenesis by acting via NMDA receptors and  $\text{Ca}_v1.2/1.3 \text{ Ca}^{2+}$  channels on the adult NPCs themselves.

If excitation-neurogenesis coupling is operative in vivo and mediates, at least in part, the effects of electrical activity on neuron production, actively dividing cells would need to exist in a cellular niche that exposes them

to network activity. The positioning of the NPCs within the axon-rich environment of the hippocampal subgranular zone seems an ideal setting (Seri et al., 2001; Filipov et al., 2003). Here, activity-dependent depolarizing mechanisms (Jefferys, 1995) could directly influence proliferating NPCs, presumably through  $\text{Ca}_v1.2/1.3$  channels, which as noted above can serve as a potent final common pathway by which electrical signals at the plasma membrane trigger activity-dependent gene expression programs (Deisseroth et al., 1998; West et al., 2001). To test this possibility in vivo, we again employed nifedipine as a potent and selective antagonist of the  $\text{Ca}_v1.2/1.3$  channels with good CNS penetration.  $\text{Ca}_v1.2/1.3$  channels do not affect hippocampal synaptic transmission (Wheeler et al., 1994), whereas other pharmaco-

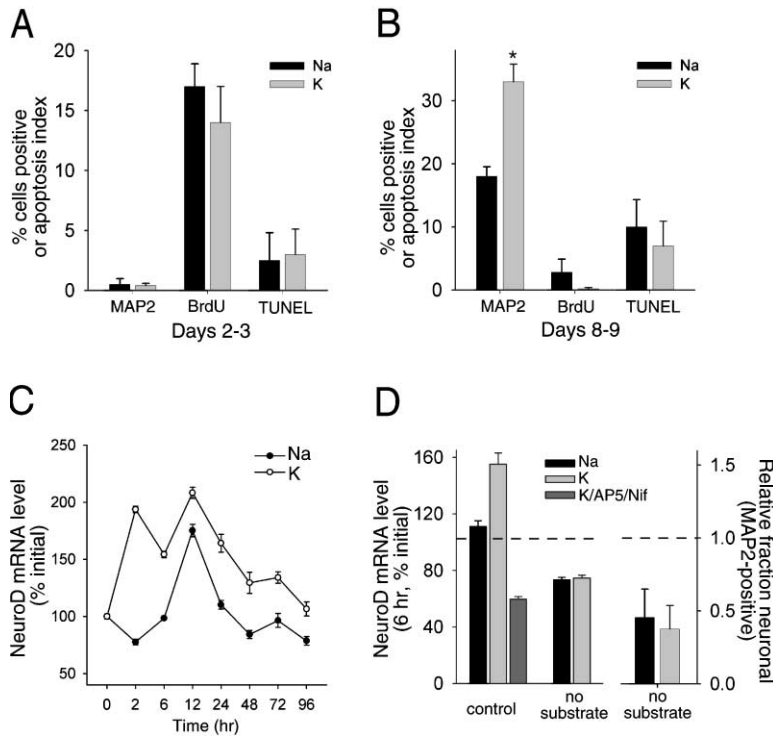


Figure 6. Excitation Acts to Induce a Proneural Response in Proliferating NPCs (A) Assessment of proliferation, survival, and differentiation during days 2 and 3 (average) in excitation or control conditions; as before, excitation begins on day 1. Mean of three independent experiments in pure NPCs growing on fixed substrate ( $p > 0.2$  for all comparisons). MAP2ab-positive cells are virtually absent within the first 2 days, demonstrating the absence of differentiated neurons; notably, it is within this 48 hr period that  $Ca^{2+}$  imaging was performed (Figures 3A and 3B). Proliferation was measured as the percent BrdU-positive cells after a brief 2 hr BrdU labeling period and immediate fixation. Apoptosis index was defined as the mean total TUNEL-positive cells observed per 20 random fields. (B) Days 8 and 9 in excitation or control conditions, as in (A). (C) Time course of *NeuroD* expression (measured by real-time PCR as with *HES1* and *Id2*) reveals a persistent elevation caused by excitation (K). Each sample was tested in four replicates, and similar results were observed in two experiments. (D) (Left) The *NeuroD* increase was blocked by the  $Ca^{2+}$  channel antagonists and not seen in the polyornithine/laminin condition without fixed hippocampal cellular substrate ("no substrate"). Dotted line represents initial control *NeuroD* level. (Right) No excitation-neurogenesis coupling occurs in the substrate environment that does not permit activity-dependent *NeuroD* induction (pooled data from three independent experiments). Dotted line indicates control unstimulated neuronal fraction with hippocampal substrate.

logical modulators such as NMDA receptor antagonists can induce unpredictable activity patterns by disinhibiting local circuits (Krystal et al., 2003).

Consistent with the *in vitro* results, *in vivo* administration of nifedipine along with BrdU labeling for 1 week significantly reduced the fraction of newborn cells assuming the neuronal phenotype, observed at the end of the labeling period ( $n = 3$ ;  $p < 0.001$ ; Figures 7C and 7D). In contrast, direct positive modulation of  $Ca_v1.2/1.3$  channels with the agonist FPL 64176 induced a relative increase in the neuronal fraction (Figures 7C and 7D).  $Ca_v1.2/1.3$  channels *in vivo* presumably respond to native patterns of hippocampal excitatory activity. Therefore, to test the effects of dampening normal endogenous activity patterns on adult neurogenesis, we examined the consequences of chronic administration of diazepam, a long-acting benzodiazepine that has been shown to cause a stable, mild reduction in net hippocampal excitatory activity (Longo et al., 1988). *In vivo* diazepam administration caused a significant reduction in the fraction of BrdU-positive cells that assumed a neuronal phenotype (Figures 7C and 7D;  $n = 3$ ;  $p < 0.002$ ). A nonsignificant trend toward an increased fraction of astroglial and oligodendroglial progeny in the conditions that inhibited neurogenesis was also observed (data not shown). While these experiments do not allow any conclusions concerning the cell type(s) upon which the drugs act or the mechanisms by which increased neurogenesis occurs *in vivo*, the results nevertheless are consistent with the hypothesis that activation of  $Ca_v1.2/1.3$  channels on adult hippocampal NPCs *in vivo* promotes neurogenesis.

Many newborn neurons die within the first 2 weeks *in vivo*, but behavioral studies of neurogenesis have implicated 2- to 4-week-old newborn neurons in certain aspects of hippocampal function (Shors et al., 2001; Feng et al., 2001; Santarelli et al., 2003). We therefore asked whether increased neurogenesis associated with  $Ca_v1.2/1.3$  channel stimulation could be detected as long as 1 month after the conclusion of the stimulation/BrdU labeling. Employing a milder agonist of  $Ca_v1.2/1.3$  channels for these long-term studies (BayK 8644), we found that increased neurogenesis could be detected 30 days after the last BrdU labeling/channel stimulation treatment. The fraction of newborn cells that were neurons was  $120\% \pm 11\%$  of control ( $p < 0.05$ ; Figure 7E), and more total newborn cells were also observed; BrdU+ cells per hippocampus (subgranular zone and hilus) measured with unbiased stereology increased from  $7,785 \pm 1,282$  in control to  $19,633 \pm 2,677$  in Bay K (2.5-fold increase,  $p < 0.005$ ). In sum, a stable increase in neuronal fraction was seen (corresponding to the pathway studied *in vitro*) and a stable increase in total newborn cells was also seen that further augments the increase in neurogenesis (likely due to recruitment of a novel pathway in the complex *in vivo* environment). These *in vivo* studies do not allow us to target a particular cell type or discriminate among altered fate, proliferation, or survival, but they do show that increased neurogenesis is a robust and stable consequence of  $Ca_v1.2/1.3$  channel activity in the intact adult brain. These data suggest that the effects of activity on NPCs *in vitro* may indeed be representative of aspects of the behavior of NPCs *in vivo* and raise the final question of what physio-

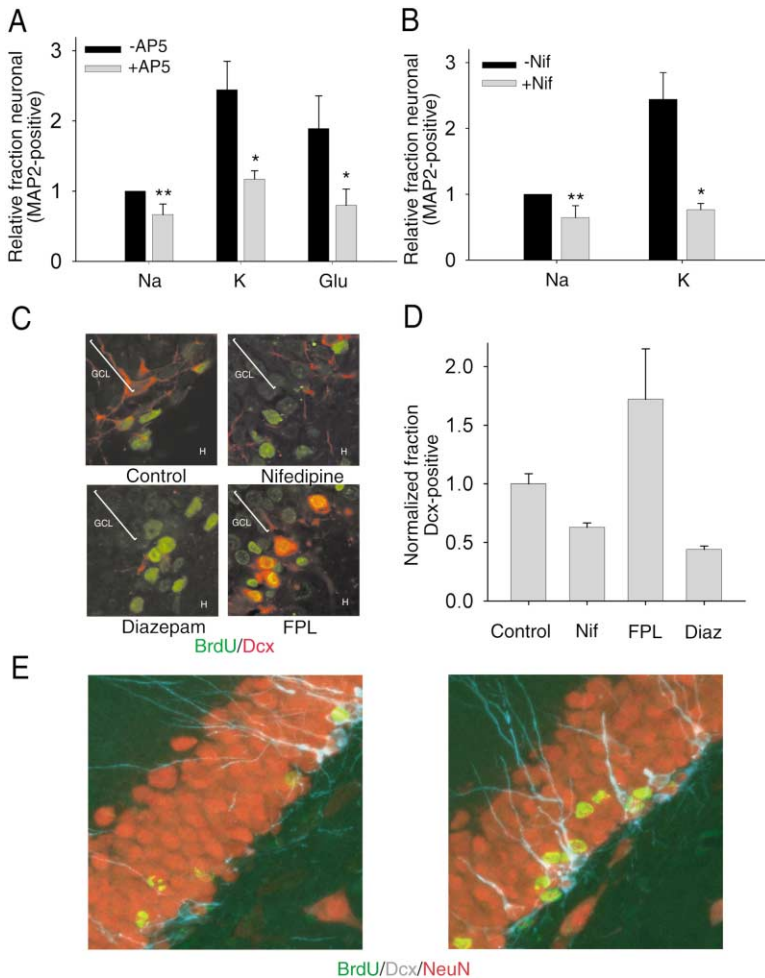


Figure 7.  $Ca^{2+}$  Channel Modulators and Activity Influence Neurogenesis in Intact Systems

(A) Living coculture model, as in Figure 2. Inhibition of NMDA receptors with D-AP5 (50  $\mu$ M) blocked excitation-induced neurogenesis via either depolarization or glutamate application. Depolarization (K),  $n = 6$  experiments; glutamate (Glu),  $n = 3$  experiments. (B) The  $Ca_v1.2/1.3$  antagonist nifedipine also inhibited basal and excitation-induced neurogenesis ( $n = 3$  experiments per condition). Drugs were provided with the differentiation medium in conjunction with the stimuli as before.

(C) Images of dentate gyrus from adult rats that received either vehicle, nifedipine, FPL 64176, or diazepam (all at 4 mg/kg) as indicated, followed by perfusion and staining for Dcx (red) and BrdU (green). Animals received daily injections for 1 week along with BrdU (50 mg/kg).

(D) Summary graph of  $Ca^{2+}$  channel modulation results. Three adult female rats were used per condition, with plotted values normalized to control neuronal fraction of 35.3% and representing the fraction of cells among those proliferating during the experimental period (BrdU+) which came to express the early neuronal phenotype (Dcx+).

(E) Rats were treated with BrdU/BayK 8644 (right,  $n = 3$ ) or BrdU/vehicle (left,  $n = 4$ ) for 1 week to label newborn cells in the context of  $Ca_v1.2/1.3$  channel stimulation, then allowed to live for 30 days prior to sacrifice. Panels show examples of merged confocal z stacks of triple labeling for BrdU/NeuN/Dcx. Many of the newborn neurons have migrated into the mature granule cell layer; yellow nuclei in both panels reveal BrdU/NeuN costaining within the GCL (array of red nuclei).

logical function could be served by this excitation-neurogenesis coupling.

### Functional Consequences of Excitation-Neurogenesis Coupling

While models of the functional impact of neurogenesis on sensory information processing within the olfactory bulb have been proposed (Cecchi et al., 2001; Petreanu and Alvarez-Buylla, 2002), current views on the role of neurogenesis within the hippocampus are inconsistent; for example, adult neurogenesis has been variously implicated in either the storage or clearance of memories (Feng et al., 2001; Shors et al., 2001). Surprisingly, using a simple network modeling approach we find that both views may be correct, as the excitation-neurogenesis coupling relationship described here can, in principle, underlie beneficial effects of adult neurogenesis in *both* memory clearance and memory storage.

Models of information storage using simple simulated neural networks have deepened our understanding of normal brain function (Graham and Willshaw, 1999; Hopfield and Tank, 1986; McClelland and Rumelhart, 1985; Sejnowski, 1999). Using a simple layered neural network (Graham and Willshaw, 1999) (Figure 8A) capable of storing and recalling many patterns of activity, we have asked whether new neurons can be usefully incorpo-

rated into mature memory processing networks and explored the advantages and disadvantages of this process in different activity regimes. We do not explore the complex question of whether insertion of a new neuron can help store the memory of the same activity that led to creation of the neuron. Instead, we have addressed the more straightforward question of how neurogenesis allows the network to adapt to different levels of memory storage demands, which in turn are correlated with the activity level in the network. In this view, activity-dependent neurogenesis may affect the *future* learning of new memories or the degradation and clearance of previously stored memories.

Full details of the model are provided in the Supplemental Data available at <http://www.neuron.org/cgi/content/full/42/4/535/DC1>. Briefly, memories (in the form of patterns of neuronal activity) are stored in the network using associative or Hebbian (Sejnowski, 1999) synaptic plasticity rules like those used in the hippocampus (e.g., when two neurons are active at the same time during exposure to an input, the efficacy of the synaptic connection between them is increased). Apart from this hippocampus-like provision, no detailed assumptions about wiring or dynamics were made, as little is known about the functional relevance of these parameters to how information is actually stored in the brain. The net-

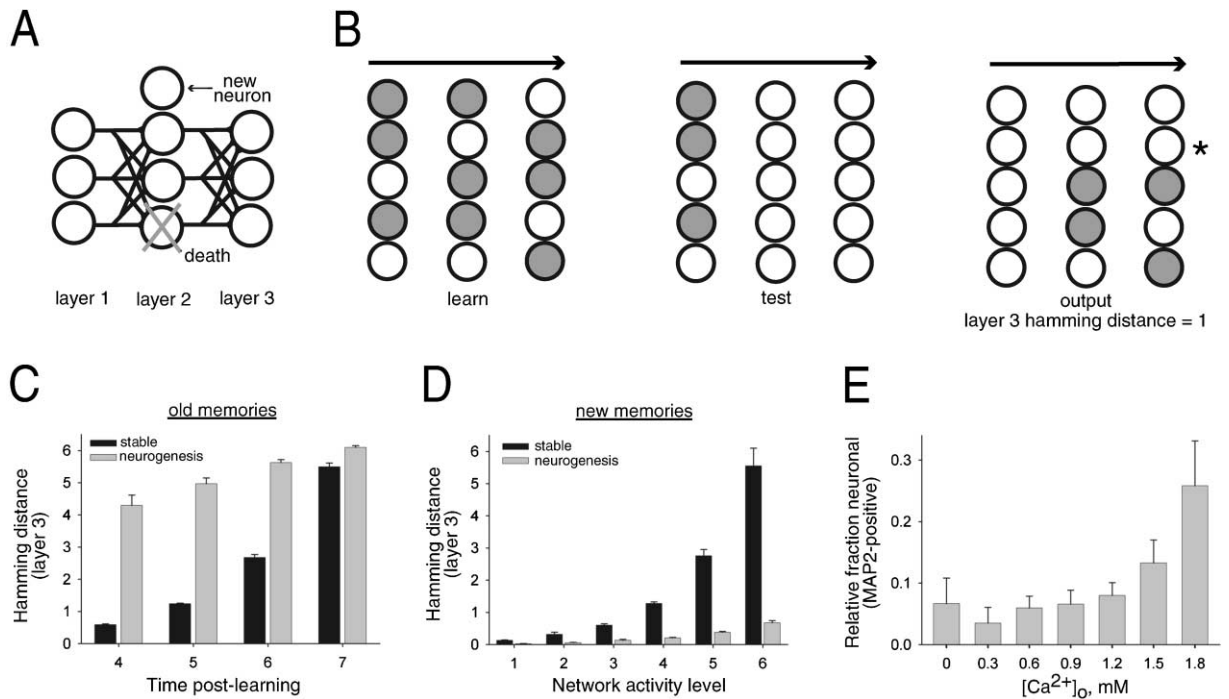


Figure 8. Functional Consequences of Excitation-Neurogenesis Coupling

(A) Diagram of the associative neural network. Key characteristics are three-layered structure, feedforward connectivity, sparse representations, and memory storage capability via use of Hebbian synapses (see Experimental Procedures and the Supplemental Data online at <http://www.neuron.org/cgi/content/full/42/4/535/DC1>).

(B) Memories are presented to the input layer (layer 1), processed by the middle layer (layer 2, where neurogenesis is also allowed to occur), and performance assessed at the output layer (layer 3). Performance is quantified as the Hamming distance, defined as the number of output units at which the actual output activity differs from the learned one for that pattern. Note the output layer neuron that is incorrectly inactive (\*), which would lead to a Hamming distance score of 1.

(C) Memory loss/clearance caused by cell turnover. Although even without turnover (stable case) old memories are increasingly lost as new memories are stored, memory loss/clearance is accelerated by the presence of balanced neurogenesis and cell death (neurogenesis case). Each unit of “time postlearning” corresponds to the learning of 50 new memories; significant degradation of old memories in the stable case begins to be apparent after time = 6, corresponding to 700 stored patterns in a network of 500 neurons per layer.

(D) High-activity networks involved in high rates of pattern storage increasingly (and monotonically) benefit from turnover. Network activity level is measured again in units of 50 stored patterns, with higher levels of pattern storage corresponding to more active networks; 500 stored patterns correspond to activity level 1 and 750 stored patterns to activity level 6. Mean values shown in bar plots represent Hamming distances averaged over all stored patterns.

(E) Experimentally determined neurogenesis increases as a monotonic function of extracellular  $[Ca^{2+}]_o$ . Steady depolarization was provided in the presence of 20 mM  $K^+$  and varying  $[Ca^{2+}]_o$ ; mean data shown from three independent experiments performed in adult NPCs plated on fixed hippocampal substrate.

work has a simple three-layered structure (Figures 8A and 8B) and can robustly store many memories in the form of activity patterns. Appropriately patterned output (i.e., memory recall, assessed by inspection of the third layer) is elicited by a patterned test stimulation of the first (input) layer. Many memories can be stored using the network synapses, but highly active networks gradually become “overloaded” and begin to display “noisy” or unreliable recall, as individual synapses attempt to satisfy the requirements of too many memories. Simple networks such as these have been widely used as models for information processing or memory storage (Graham and Willshaw, 1999; Hopfield and Tank, 1986; McClelland and Rumelhart, 1985; Sejnowski, 1999).

We compared the function of a control, stable network to a network in which neurogenesis occurs in only the middle layer (as is thought to occur in vivo in the dentate gyrus; steady addition of new neurons was balanced by steady loss of existing neurons, keeping network size

unchanged). We observed two key network behaviors relating to memory clearance and memory storage. First, we found that neurogenesis elicited a more rapid loss or clearance of previously stored old memories (Figure 8C). To some extent this may be expected, as the synapses of the new neurons have no access to information on the old memories formed before their birth, and the turnover of old neurons coupled with behavior of the new neurons therefore can only degrade the network’s ability to recall old memories. This aspect of the model may provide a quantitative framework for understanding how a balance of neuron loss and replacement could be important for the clearance of previously stored memories (Feng et al., 2001), perhaps especially so in a network that had been very active and is heavily overloaded with old memories.

Second, with regard to the storage of new memories, we found that the newest memories were recalled at a higher fidelity (compared to the zero-neurogenesis sta-

ble case) when neurogenesis was allowed to occur (Figure 8D), despite the fact that total network size was not allowed to increase. This effect can be intuitively understood from the lack of involvement of new neurons in old memories; in effect, their synapses can be devoted more fully to the newer memories, which are then more accurately stored. Critically, this advantage was dramatically greater in networks that had been more active and had been required to store many memories (Figure 8D) by comparison with the low activity (low storage rate) networks. This conditional advantage of neurogenesis for memory storage in heavily active networks predicts a monotonically increasing function linking network activity level to the relative benefits of neurogenesis in memory storage (Figure 8D). Note that this advantage does not depend on a particular mechanism for excitation-neurogenesis coupling.

Importantly, such a relationship was in fact found experimentally in the excitation-neurogenesis coupling characteristics of the adult NPCs (Figure 8E). Because both NMDA receptors and  $\text{Ca}_v1.2/1.3$  channels mediate their long-lasting effects through  $\text{Ca}^{2+}$  flux, we tested the dependence of neurogenesis on  $\text{Ca}^{2+}$  by varying external  $[\text{Ca}^{2+}]$  in the setting of depolarization in the fixed coculture substrate condition (Figure 8E). As external  $[\text{Ca}^{2+}]$  was increased over a broad range up to 1.8 mM, neurogenesis monotonically increased, indicating that within this range a monotonic relationship with positive slope exists between external  $\text{Ca}^{2+}$  and the extent of neurogenesis. Since there were no living cells present except for the NPCs, these experiments demonstrate that processing mechanisms within the NPCs themselves can in principle implement the simple rules governing the excitation-neurogenesis coupling that had been predicted from network modeling. Further work will be needed to define the excitation-neurogenesis coupling function in vivo, particularly as related to different levels of behaviorally relevant hippocampal activity.

## Discussion

### Excitation-Neurogenesis Coupling: An Intrinsic Property of Proliferating Adult NPCs

Using an array of approaches, we have explored the coupling of excitation to neurogenesis in proliferating adult-derived NPCs, both in vitro and in vivo. Adult neurogenesis is potentially enhanced by excitatory stimuli and involves  $\text{Ca}_v1.2/1.3$  channels and NMDA receptors. These  $\text{Ca}^{2+}$  influx pathways are located on the proliferating NPCs, allowing them to directly sense and process excitatory stimuli. We found no effect of excitation on extent of differentiation in individual cells (measured by extent of MAP2ab expression in the NPC-derived neurons) nor did we observe effects on proliferative rate or fraction, survival, or apoptosis. Instead, excitation increased the fraction of NPC progeny that were neurons, both in vitro and in vivo, and total neuron number was increased as well. The  $\text{Ca}^{2+}$  signal in NPCs leads to rapid induction of a proneural gene expression pattern involving the bHLH genes *HES1*, *Id2*, and *NeuroD*, and the resulting cells become fully functional neurons defined by neuronal morphology, expression of neuronal structural proteins (MAP2ab and Doublecortin), expres-

sion of neuronal TTX-sensitive voltage-gated  $\text{Na}^+$  channels, and synaptic incorporation into active neural circuits. A monotonically increasing function characterizes excitation-neurogenesis coupling, and incorporation of this relationship into a layered Hebbian neural network suggests surprising advantages for both the clearance of old memories and the storage of new memories. Taken together, these results provide a new experimental and theoretical framework for further investigation of adult excitation-neurogenesis coupling.

In the hippocampal formation, neural stem cells exist either within the adjacent ventricular zone or within the subgranular zone proper at the margin between the granule cell layer and the hilus, where proliferative activity is most robust (Seaberg and van der Kooy, 2002; Seri et al., 2001; Filippov et al., 2003). These cells do not express neuronal markers but proliferate and produce dividing progeny that incrementally commit to differentiated fates (such as the neuronal lineage) over successive cell divisions (Kempermann et al., 2003). Native NPC populations in vivo are therefore heterogeneous with regard to lineage potential, and we lack markers that distinguish between the multipotent stem cell and the subtly committed yet proliferative progenitor cell. Excitation may therefore act on either or both types of proliferating precursor, in vitro and in vivo. The functional consequences of coupling excitation to insertion of new neurons for the neural network, however, is independent of which precursor cell types respond to excitation.

### $\text{Ca}^{2+}$ Influx Pathways: Ion Channels Involved in Excitation-Neurogenesis Coupling

$\text{Ca}_v1.2/1.3$  channels on adult NPCs potentially influenced neurogenesis, as the specific agonists (FPL 64176 and BayK 8644) and antagonist (nifedipine) bidirectionally modulated excitation-neurogenesis coupling in vivo and in vitro.  $\text{Ca}_v1.2/1.3$  channels are classified among the high voltage-activated (HVA)  $\text{Ca}^{2+}$  channels, and in mature neurons, these channels open primarily in response to the depolarization provided by excitatory synaptic inputs. Measurements of resting potential have indicated that neural precursors can maintain resting potentials in the  $-55$  mV range (Wang et al., 2003), and both the bHLH gene response and calcium imaging reported here are consistent with successful membrane depolarization and  $\text{Ca}^{2+}$  channel activation in the NPCs. For proliferating NPCs in vivo, which presumably are not synaptically connected, these channels may be activated by a number of other mechanisms. First,  $\text{Ca}_v1.2/1.3$  channels may be partially open at rest, since NPCs tend to be more depolarized than mature quiescent neurons (Wang et al., 2003; Westerlund et al., 2003). Supporting this hypothesis, we found inhibition of neurogenesis by nifedipine even in the resting, nonstimulated condition. The relative resistance to inactivation that characterizes  $\text{Ca}_v1.2/1.3$  compared to other HVA channels (Tsien et al., 1995) makes them well-suited to this type of chronic signaling (See et al., 2001; Mao et al., 1999). Additional nonsynaptic depolarizing influences could come into play in the densely packed in vivo cellular milieu in which NPCs are found. These include depolarizing responses to extracellular  $[\text{K}^+]$ , which increases during bouts of local neuronal activity (Gardner-Medwin

and Nicholson, 1983; Malenka et al., 1981), and depolarizing (ephaptic) responses to voltage changes in active neighboring neurons (Jefferys, 1995).

Second, the NPCs could also express depolarizing receptors that can function without classical synaptic contacts. Chief among these possibilities, the NMDA receptor (which passes both  $\text{Ca}^{2+}$  and  $\text{Na}^+/\text{K}^+$ ) can have a powerful depolarizing influence and has a very high affinity for glutamate, allowing detection of "ambient" or extrasynaptic glutamate (Sah et al., 1989), the levels of which change in response to activity. Indeed, NMDA receptors also were found to be important in excitation-neurogenesis coupling in adult NPCs, as the antagonist D-AP5 and agonists NMDA and glutamate bidirectionally regulated neurogenesis.

#### **A Gene Expression Pattern Triggered by Excitation in Proliferating Adult NPCs**

Excitation required target cells to be proliferating for effects on neurogenesis to be observed, as excitation provided after cell cycle exit had no effect on neuron abundance. Conversely, excitation provided as a short (5 min) pulse when >90% of NPCs were known to be proliferating gave rise to significantly increased neurogenesis. These findings led to the question of whether proliferating NPCs could respond to excitation with an appropriate transcriptional response. To address this issue, we used real-time PCR to quantify the effects of excitation on the expression levels of several key bHLH genes in the proliferating adult NPCs. Excitation indeed caused rapid induction of a gene expression pattern characterized by decreases in expression of the antineuronal phenotype genes *HES1* and *Id2* and a rapid and stable increase in the expression of the downstream neuronal differentiation regulator *NeuroD*. Antagonism of  $\text{Ca}_v1.2/1.3$  channels and NMDA receptors blocked the excitation-induced responses of all three bHLH genes, providing an independent assay for the ability of  $\text{Ca}^{2+}$  influx to couple effectively to intracellular signaling pathways in adult NPCs. Evidence for the functional importance of these molecular responses in excitation-neurogenesis coupling was provided by the demonstration that preventing the activity-dependent downregulation of *Id2* prevented the normal excitation-induced increase in neurogenesis. Further work is required to determine how these bHLH genes are regulated by activity.  $\text{Ca}^{2+}$  signaling through  $\text{Ca}_v1.2/1.3$  channels and NMDA receptors can activate a broad array of rapidly responsive transcription factors, including CREB, NF-ATc4, NF- $\kappa$ B, MEK2, c-fos, and others (Deisseroth et al., 2003). Moreover, excitation could in principle induce release of autocrine factors from the NPCs themselves, leading to recruitment of a host of additional signaling pathways to nuclear transcription factors.

#### **Environmental Control of Excitation-Neurogenesis Coupling**

Our findings are consistent with the principle that local cellular environments are important in controlling neurogenesis and, in particular, with the recent demonstration that hippocampal coculture promotes hippocampal neurogenesis (Song et al., 2002). Indeed, we found that adult NPCs grown in an environment nonpermissive for

neurogenesis were unable to respond to excitation. It will be of great interest to determine the factor(s) present in the fixed hippocampal substrate condition that permit this excitation-neurogenesis coupling to occur; presumably, a surface molecule on native hippocampal cell membranes is able to induce competence in the NPCs.

Cells with neurogenic potential exist elsewhere in the brain as well (Alvarez-Buylla and Garcia-Verdugo, 2002), including neocortex (Palmer et al., 1999; Gould et al., 2001), but contribute to neurogenesis only in the subventricular zone and the dentate gyrus subgranular zone. However, when cells from nonneurogenic areas are removed and transplanted into neurogenic areas, neuronal progeny result (Palmer et al., 1999; Suhonen et al., 1996; Shihabuddin et al., 2000). Our results suggest that one contributing factor to the different neurogenic potential of different brain areas may be differences in the ability of local neuronal activity to induce competence for excitation-neurogenesis coupling in the resident population of NPCs, just as differences in local astroglia (Song et al., 2002) can also contribute. Whether this regional variation might be due to local activity patterns, access of resident NPCs to the local activity (Seri et al., 2001; Filippov et al., 2003), ability of the local environment to induce activity-sensing competence in the NPCs, or factors intrinsic to the resident NPCs themselves, remains to be determined.

The enhancement of hippocampal neurogenesis by behavioral stimuli such as environmental enrichment and running (van Praag et al., 1999) may, at least in part, be implemented at the molecular level by excitation-neurogenesis coupling. Notably, running and environmental enrichment increase adult neurogenesis in the hippocampus but not in the subventricular zone (Brown et al., 2003). Of course, not every neurogenic region in the brain need follow the excitation-neurogenesis coupling rule outlined here. An activity rule appropriate for the unique information processing or storage function of that brain region might be expected to operate. In this context, it is interesting to note that, while subventricular zone/olfactory bulb precursor neurogenesis is not enhanced by behavioral activity, proliferation and survival in this system can be influenced by olfactory sensory stimuli (Rochefort et al., 2002). This suggests that a different form of activity rule, appropriate for that local circuit, may govern olfactory bulb neurogenesis (Petreanu and Alvarez-Buylla, 2002; Cecchi et al., 2001).

#### **Significance for Hippocampal Functioning**

Adult excitation-neurogenesis coupling could be a special adaptation with a unique information processing purpose. In the model neural network (Figure 8), this single phenomenon surprisingly promoted both the clearance of old memories and the storage of new memories, precisely the two roles to which adult neurogenesis has been experimentally linked (Feng et al., 2001; Shors et al., 2001). (A recent network model that stored alphabetic character representations [Chambers et al., 2004], published after review of this paper, also reached similar conclusions.) Indeed, the  $\text{Ca}^{2+}$  influx pathways shown here to be important for excitation-neurogenesis coupling also contribute to synaptic plasticity and presumably stable memory formation in mammals (Bear

and Malenka, 1994). The existence of excitation-neurogenesis coupling may be particularly important in the hippocampus, a heavily-used locus for temporary memory storage (Kandel, 2001; Squire and Zola-Morgan, 1991), where frequent memory turnover heightens the need for efficient means of eliminating old memories while reliably storing new memories. Adult excitation-neurogenesis coupling need not even be a constitutive property of NPCs in the hippocampus, as neurogenesis might exist in modes that are switched on or off by neuromodulatory inputs. Ideally, progenitors would be able to use modulatory inputs to distinguish activity relating to new memory storage (which should trigger neurogenesis) from activity relating only to the use of old memories (which should not necessarily lead to a requirement for more neurons, as there is not increasing memory load placed on the circuits).

The effect of  $Ca_v1.2/1.3$  channel stimulation on the fraction of newborn neurons identified *in vitro* was also observed *in vivo* and found to produce an increase in the number of new neurons that was stable for at least 1 month. *In vitro*, where NPC-intrinsic mechanisms could be examined in the absence of living neurons and glia, we found that depolarization of the NPC itself did not impact proliferation or cell death. *In vivo*, the NPC is surrounded by a wide variety of neurons, glia, microglia, and vascular cells, each of which is known to influence NPC activity and fate. The cumulative effects of  $Ca^{2+}$  channel stimulation on each of these cell types could have yielded effects that were completely contrary to the *in vitro* data, yet the net result of  $Ca_v1.2/1.3$  channel excitation *in vivo* was in fact a robust and stable promotion of neurogenesis. This result indicates that NPC regulatory mechanisms may be coordinately managed within the complex environment of the subgranular zone.

Manipulation of activity *in vivo* may have important clinical implications (Bjorklund and Lindvall, 2000), particularly as NPCs can invade regions of damaged brain tissue following stroke or ischemia (Arvidsson et al., 2001; Nakatomi et al., 2002), and in some circumstances can contribute to long-range connections and functional recovery (Arvidsson et al., 2001; Park et al., 2002). It is conceivable that pharmacological interventions or manipulations of neural activity could enhance the ability of either native or transplanted NPCs to restore function to damaged areas of the CNS. Electroconvulsive therapy (ECT), as used for the treatment of psychiatric and neurological disorders, is particularly intriguing along these lines and involves brief  $\sim 1$  min induced seizures (global excitatory activity) provided every other day. This therapeutic pattern is similar to the pulse pattern provided in Figure 4B, suggesting that ECT could be adapted to specifically promote neurogenesis (Madsen et al., 2000; Malberg et al., 2000; Parent et al., 1997).

Activity-dependent proliferative bursts in the dentate gyrus can be caused by other clinically relevant phenomena as well, including ischemia and seizure, which both cause acutely increased local excitation (Arvidsson et al., 2001; Gould et al., 2000; Liu et al., 1998). The excitation-neurogenesis coupling relationship described here may help guide the neurogenesis observed after such proliferative bursts. However, the observation that brief NMDA receptor blockade induced robust stem/

progenitor cell proliferation (Cameron et al., 1995) might seem to be in conflict with the present results, which demonstrate that stimulation of NMDA receptors increases neurogenesis (Figure 3). The two sets of results in fact can be viewed as compatible, since after clearance of the NMDA receptor antagonist, neuronal activity would presumably return to appropriate levels, allowing excitation during the proliferative burst to promote neuronal fate selection. Additionally, NMDA receptor antagonists *in vivo* can produce excitatory activity patterns by disinhibiting local circuits (Krystal et al., 2003), which would further support increased neurogenesis. Such a mechanism may be particularly important in light of the fact that excess glutamate leading to NMDA receptor activity can be toxic to mature neurons; linking the same excess glutamate to the production of new neurons would presumably be of adaptive value for the organism. It will be important to conduct further mechanistic work in reduced preparations, to identify specific ways by which adult NPCs might be guided to incorporate into damaged or overloaded neural circuits *in vivo*.

#### Experimental Procedures

##### *In Vivo* Neurogenesis Assays

Adult 160 g female Fisher rats were injected once per day over a 6 day period with BrdU (50 mg/kg *i.p.* in 0.9% saline) along with drug or vehicle control (1% Tween-80/1% ethanol; drug and vehicle injections were over 7 days, initiated 1 day before the BrdU injections commenced), anesthetized (0.75 mg/kg acepromazine, 80 mg/kg ketamine, and 20 mg/kg xylazine in saline), and sacrificed on the 7th or 37th day after BrdU initiation by transcardial perfusion with chilled 4% paraformaldehyde in PBS, followed by overnight postfixation via submersion in 4% PFA/PBS. FPL 64176, nifedipine, and diazepam were all dosed at 4 mg/kg in an injection volume of 1.6 ml, diluted from 50x stocks, and BayK 8644 was dosed at 1 mg/kg. All treatments were tolerated, with the exception of FPL 64176, as previously reported (Jinnah et al., 2000). Although the low dose used did not lead to overt dystonias, two of the FPL 64176-treated animals died shortly before sacrifice on the 7th experimental day. The brains of these two animals were removed and coronally sliced to expose the hippocampus; fixation by 4% PFA/PBS submersion overnight and subsequent staining was quantitatively indistinguishable from the FPL 64176/transcardially perfused condition. For this reason, the milder agonist Bay K8644 was used for the long-term survival studies. Following fixation, brains were immersed in 30% sucrose/ $dH_2O$  for 4 days; 40  $\mu$ M sections were cut and stored in HistoPrep cryoprotectant. Floating sections were rinsed in TBS followed by block for 30 min in 0.3% Triton X-100 and 3% Normal Donkey Serum in TBS (TBS++). Primary antibody staining was conducted in TBS/1% Normal Donkey Serum/0.3% Triton X-100 overnight at 4°C on a rotary shaker. Primary antibodies used were goat anti-Doublecortin (1:500, Santa Cruz Biotechnology) and rat anti-BrdU (1:500, Accurate). Sections were then rinsed three times in TBS, followed by overnight incubation in fluorophore-conjugated secondary antibody (1:1000) staining in TBS++. Sections were again rinsed three times in TBS and postfixated for 10 min at room temperature in 4% PFA/PBS, rinsed one time in 0.9% saline, denatured for 30 min at 37°C in 2 M HCl, rinsed in TBS, blocked, and stained as above for BrdU, aligned on slides in 50 mM phosphate buffer, partially dried, mounted, and coverslipped in 125  $\mu$ l polyvinyl alcohol-DABCO. Unbiased stereological analysis with Abercrombie correction was employed to measure total BrdU+ cell number and total hippocampal volume as previously described (Monje et al., 2002); no significant effects on hippocampal volume were observed.

##### Adult NPC Line Derivation and Culture

Hippocampus-derived NPCs were isolated from adult rat hippocampi and cultured using an adaptation of the Percoll buoyancy fraction method (Palmer et al., 1997). Briefly, adult 6- to 8-week-

old female Fisher-344 rats were deeply anesthetized, brains were removed and were dissected immediately. Hippocampi were enzymatically dissociated with papain (2.5 U/ml; Worthington, Freehold, NJ)-dispase II (1 U/ml; Boehringer Mannheim, Indianapolis, IN)-DNase I (250 U/ml, Worthington) solution. Digested tissue was then washed with DMEM-10% fetal calf serum (FCS) and subsequently mixed with isotonic Percoll solution (Amersham Pharmacia Biotech, Uppsala, Sweden) to a final concentration of 35% isotonic Percoll. The 100% isotonic Percoll solution was made by mixing nine parts of Percoll with one part of  $10 \times$  PBS. The cell suspension was then fractionated by centrifugation for 10 min at  $1000 \times g$ . Floating myelin and tissue debris were discarded and the cell pellet resuspended in 65% Percoll solution and fractionated again by centrifugation for 10 min at  $1000 \times g$ . The floating neural progenitors were collected, washed free of Percoll, and plated onto poly-L-ornithine/laminin-coated dishes in DMEM/F12 (1:1) containing 10% FCS medium for 24 hr; then medium was replaced with serum-free growth medium consisting of DMEM/F12 (1:1) supplemented with N2 supplement (Invitrogen, Gaithersburg, MD) and 20 ng/ml of human recombinant FGF-2 (Peprotech, Rocky Hill, NJ). Cell lines were labeled via infection with replication-deficient GFP-expressing recombinant retrovirus, NIT-GFP (Palmer et al., 1999) or LZRS-CAMut4GFP (Okada et al., 1999). The majority of experiments with HC37 cells transduced with NIT-GFP were conducted at passage number  $\sim 25$ . Cell lines were propagated in DMEM/F12 with 20 ng/ml bFGF, penicillin/streptomycin/amphotericin B (Life Technologies), and N2 supplement (Life Technologies). Plastic tissue culture-treated dishes were coated with 10  $\mu$ g/ml polyornithine in dH<sub>2</sub>O overnight under UV illumination, rinsed two times with dH<sub>2</sub>O, recoated with 5  $\mu$ g/ml mouse laminin (Invitrogen), incubated overnight at 37°C, and frozen for long-term storage at  $-80^\circ\text{C}$ . Cells were fed every 2–3 days by 75% solution exchange and split 1:4 every 6–7 days after brief trypsinization and centrifugation. Freezing was in DMEM/F12/10% DMSO/BIT supplement (StemCell Technologies), and thawing from storage was in DMEM/F12/BIT.

#### Hippocampal Cell Culture

Hippocampi of postnatal day 0 (P0) Sprague-Dawley rats were removed and treated with papain (20 U/ml) for 45 min at 37°C. The digestion was stopped with 10 ml of MEM/Earle's salts without L-glutamine along with 20 mM glucose, Serum Extender (1:1000), and 10% heat-inactivated fetal bovine serum containing 25 mg of bovine serum albumin (BSA) and 25 mg of trypsin inhibitor. The tissue was triturated in a small volume of this solution with a fire-polished Pasteur pipette, and  $\sim 100,000$  cells in 1 ml plated per coverslip in 24-well plates. Glass coverslips (prewashed overnight in HCl followed by several 100% EtOH washes and flame sterilization) were coated overnight at 37°C with 1:50 Matrigel (Collaborative Biomedical Products, Bedford, MA). Cells were plated in culture medium: Neurobasal containing 2x B-27 (Life Technologies) and 2 mM Glutamax-I (Life Technologies). One-half of the medium was replaced with culture medium the next day, giving a final serum concentration of 1.75%. For lightly fixed tissue experiments, stem/progenitor cells were plated after hippocampal cultures at 7 DIV were exposed to 70% EtOH at  $-20^\circ\text{C}$  for 30 min, then washed twice in sterile PBS. The NPCs were plated on the fixed substrate in 25% conditioned medium from the neuron/glia culture and 75% culture medium, as in coculture experiments (see below).

#### Stem Cell Coculture

Seventy-five percent of the medium was removed from each well of the hippocampal cultures and replaced with a coculture solution consisting of Neurobasal/B27/penicillin/streptomycin/glutamine and 20 ng/ml each of VEGF and PDGF (both from Peprotech). NPCs cultured in growth medium were treated with trypsin, washed, and added to the culture as a single cell suspension. After 1 day of attachment to substrate, the coculture was gradually adapted to differentiation medium containing 2% fetal bovine serum, 0.5  $\mu$ M all-trans retinoic acid (prepared freshly on day of use), 10  $\mu$ M forskolin, and 20 ng/ml NT3 by three 75% medium exchanges every other day. Mitotic inhibitor FUDR (5-fluoro-2'-deoxyuridine) was included with uridine at 0.3 mM unless otherwise indicated at the start of the sixth day postplating to allow for long-term culture.

Thereafter, cultures were supplemented with NT3 to 20 ng/mL every 2–3 days until cocultures were 9–16 days old (control and experimental conditions were always conducted in parallel and therefore were age matched at all times).

#### Excitation of NPCs in Coculture

Stimuli were started on day 1 along with the initiation of mitogen taper and were included in the three 75% solution exchanges: added 50  $\mu$ M glutamate, added 16 mM KCl, or added 16 mM NaCl as an osmotic control. As Neurobasal medium already contains 4 mM KCl, the potassium concentration rises to 19.75 mM after the final medium exchange. Divalent cation concentration was maintained constant in external calcium variation experiments by replacement with equimolar magnesium. Nifedipine (RBI) was used at 10  $\mu$ M and FPL 64176 at 5  $\mu$ M. Persistent stimuli were used, except where noted, to mimic areas of local persistent high activity and to avoid rebound or washoff effects. For brief stimuli, sham medium changes were conducted for control purposes with no neurogenic effect, and medium was fully replaced for the stimulation and removal of stimulation.

#### Electrophysiology

Electrophysiology was carried out essentially as described (Deisseroth et al., 1996). Whole-cell recordings were obtained with an Axopatch 1D amplifier (Axon Instruments), NIDAQ National Instruments A/D board, and Igor Pro acquisition software. Cells were visualized on an inverted Nikon microscope with mercury arc lamp attachment. Morphologically, the most neuronal GFP+ cells (phase-bright somata with two to five primary processes) present in each condition were selected for recording. For miniature EPSC acquisition, cells were held at  $-70$  mV in voltage clamp; for evoking sodium currents, cells were held at  $-70$  mV and stepped to  $-10$  mV. The chamber was perfused with Tyrode's solution containing 129 mM NaCl, 5 mM KCl, 2 mM CaCl<sub>2</sub>, 1 mM MgCl<sub>2</sub>, 30 mM glucose, 25 mM HEPES, and 10  $\mu$ M glycine (pH 7.3 and osmolarity  $313 \pm 2$  mOsm). Whole-cell patch electrodes (3–8 M $\Omega$  resistance) were filled with a solution containing 110 mM CsMeSO<sub>4</sub>, 5 mM MgCl<sub>2</sub>, 10 mM NaCl, 0.6 mM EGTA, 2 mM ATP, 0.2 mM GTP, and 40 mM HEPES (pH 7.2,  $295 \pm 2$  mOsm), unless otherwise noted. TTX (from Calbiochem) at 1  $\mu$ M was applied and washed via custom-designed perfusion pipes positioned by the patched cell.

#### Immunocytochemistry and Transfection

Cells were fixed in 4% formaldehyde (EM Sciences)/PBS for 20–30 min, washed  $3 \times 5$  min in PBS/0.1M glycine, permeabilized for 5 min in 0.1% Triton/PBS/3% BSA, washed  $3 \times 5$  min in PBS/glycine, blocked for 1–2 hr in PBS/3% BSA, and incubated overnight at 4°C in PBS/3% BSA/primary antibodies. Cells were then washed  $3 \times 5$  min in PBS, incubated for 1 hr at 37°C in PBS/3% BSA/secondary antibodies, washed  $3 \times 10$  min in PBS, and mounted in Fluoromount (Electron Microscopy Sciences). TUNEL staining was performed with Apoptag Red (Serologicals). MAP2ab monoclonal Ab clone AP20 (Sigma) was used at 1:500, Doublecortin Ab (Santa Cruz Biotechnology) at 1:750, BrdU Ab (Accurate) at 1:500, NeuN at 1:4, and secondary Abs from Jackson ImmunoResearch at 1:1000. Cotransfections were carried out with Lipofectamine 2000 according to the manufacturer's instructions immediately after NPC plating. The pIRES-EGFP-Id2 plasmid (with CMV promoter) was obtained from Ben Barres, Stanford University; GFP expression is low from this IRES, and cotransfection with DsRed (Clontech) was used to identify transfected cells. Approximately 2%–5% of the NPCs were transfected, and results shown therefore represent mean MAP2ab levels from all DsRed-positive cells in each condition rather than neuronal fraction obtained from a histogram. As with all experiments, stimulation or control conditions were initiated 24 hr after transfection on day 1.

#### Confocal Imaging and Analysis

Images were acquired on a Zeiss LSM confocal microscope. Random fields containing GFP+ cells were selected for acquisition under GFP excitation without knowledge of experimental condition. MAP2ab or Dcx fluorescence values were obtained for each GFP+ cell by quantifying the mean intensity of the corresponding fluoro-

phore pixels overlying GFP<sup>+</sup> pixels; occasional cells were excluded during analysis if they were found to be overlaid with MAP2ab-positive processes from other nearby cells. Histograms of resulting values were generated for each experiment, and MAP2ab-positivity threshold values for the fractional neurogenesis criterion were identified from the histograms, which show in the unstimulated case (as in Figure 2) a sufficiently bimodal character allowing a threshold expression level to be set. Mean data from 12 independent experiments conducted with potassium depolarization were used as the reference point for effects of pharmacological interventions in coculture. For evaluation of proliferation and survival effects, BrdU was applied to cultures at 5  $\mu$ M for 2 hr, and BrdU staining was conducted with a 20–30 min postfixation and subsequent incubation at 37°C for 20–30 min in 1 N HCl. For Ca<sup>2+</sup> imaging, x-Rhod-1 AM (Molecular Probes) was loaded at 10  $\mu$ M for 30 min at 37°C into cells on the fixed coculture substrate 1–2 days after initiation of mitogen taper. Solutions for resting and stimulated cases corresponded to the differentiation solutions described above, and values shown represent mean somatic x-Rhod-1 fluorescence averaged over all observed cells. 100% of the cells imaged are represented in the averages.

#### Total RNA Isolation, cDNA Synthesis, and SYBR Green Real-Time Quantitative RT-PCR

Total RNA was isolated using RNeasy mini kit (Qiagen), and synthesis of cDNA was performed using the SuperScript First-strand Synthesis System for RT-PCR (Invitrogen) following the manufacturers' instructions. Quantitative SYBR Green real-time PCR was carried out as described previously (Mitrasinovic et al., 2001). Briefly, each 25  $\mu$ l SYBR green reaction consisted of 5  $\mu$ l of cDNA (50 ng/ $\mu$ l), 12.5  $\mu$ l of 2x Universal SYBR Green PCR Master Mix (PerkinElmer Life Sciences) and 3.75  $\mu$ l of 50 nM forward and reverse primers. Optimization was performed for each gene-specific primer prior to the experiment to confirm that 50 nM primer concentrations did not produce nonspecific primer-dimer amplification signal in no-template control tubes. Primer sequences were designed using Primer Express Software. Quantitative RT-PCR was performed on ABI 5700 PCR instrument (PerkinElmer Life Sciences) by using three-stage program parameters provided by the manufacturer as follows; 2 min at 50°C, 10 min at 95°C, and then 40 cycles of 15 s at 95°C and 1 min at 60°C. Specificity of the produced amplification product was confirmed by examination of dissociation reaction plots. A distinct single peak indicated that a single DNA sequence was amplified during PCR. In addition, end reaction products were visualized on ethidium bromide-stained 1.4% agarose gels. Appearance of a single band of the correct molecular size confirmed specificity of the PCR. Primers were as follows (F, forward; R, reverse): GAPDH F, AAGAGAGAGGCCCTCAGTTGCT; GAPDH R, TTGTGAGGGAGATG CTCAGTGT; MASH1 F, GACAGGCCCTACTGGGAATG; MASH1 R, CGTTGTCAAGAACAACCTGAAGACA; HES1 F, CGGCTTCAGCGAG TGCAT; HES1 R, CGGTGTTAACGCCCTCACA; HES5 F, GGAGGCG GTGCAGTTCCT; HES5 R, GGAGTGGTAAAGCAGCTTCATC; ID2 F, ACAACATGAACGACTGCT; ID2 R, ATTTCCATCTTGGTCACC; NEUROD F, GGACAGACGAGTGCCTCAGTTC; NEUROD R, TCATGGCT TCAAGCTATCCTCCT.

#### Layered Hebbian Neural Network

Key characteristics of the model network are noted below; C source code is available on request. The aim of the model is to explore the effects that excitation-neurogenesis coupling could have on a memory-storage neural network (and not to precisely mimic a particular preparation, though key parallels to hippocampal functioning are included). The network consists of three layers with feedforward, full synaptic connectivity; the output layer activity pattern can be readily conceived of as a stable equilibrium of neuronal activity (according to some theories, analogous to the brain state during active remembering), for example, with neurons therein capable of persistent activity or participating in simple recurrent connections.

In the results presented, there were 500 neurons per layer, and neurogenesis with cell turnover was permitted only at the middle "dentate gyrus" layer. For modeling clearance of old memories in Figure 8, turnover fraction was 0.05 for every 50 new patterns stored;

for cell death, neurons were selected randomly. As newborn neurons must make functional connections in order to learn, such new neurons were allowed full connectivity to the presynaptic and postsynaptic layers after being born and were allowed to learn subsequent patterns like the other neurons.

Synaptic connections were excitatory, and neurons were simple threshold elements with binary activation values  $\xi = 0$  or 1. As in the hippocampus, pattern representations were sparse; fraction of active neurons per pattern or sparsity ( $\alpha$ ) = 0.02 in all layers. Synaptic weights  $J$  between neurons  $i$  and  $j$  were set with the standard Hebb rule (Graham and Willshaw, 1999; Willshaw et al., 1969),  $J_{ij} = \sum(\xi_i \times \xi_j)$ , summed over all stored patterns. Activity was propagated through the network in the usual manner, with only the first layer of each stored pattern provided (via the input layer) and activity of the second and third layer determined iteratively as the network attempts to reconstruct the full memory. A given cell  $j$  was determined to be active in a reconstructed memory if the incoming activity  $\sum(\xi_i \times J_{ij})$  summed over all presynaptic neurons  $i$  into that cell exceeded a threshold  $\theta_j = \alpha_i \times n_i$ , where  $n_i$  is the total number of neurons in the  $j - 1$  layer and  $\alpha_i$  is the sparsity of the  $j - 1$  layer. Efficacy of memory recall was judged by similarity of the output (third layer) activity pattern compared with the actual stored pattern; each incorrectly active or incorrectly inactive neuron increments the Hamming distance error metric by one unit.

Full details are given in the Supplemental Data available online at <http://www.neuron.org/cgi/content/full/42/4/535/DC1>.

#### Acknowledgments

We acknowledge support from the Medical Scientist Training Program (S.S.), the Stanford Department of Neurosurgery (H.T., M.M., T.D.P.), and grants from the NIH (R.C.M., M.M., H.T., T.D.P.). We thank Xiang Yu, Mark Schnitzer, and Eric Wexler for helpful discussions. We are also grateful to Ben Barres for the *Id2* plasmid and to Greer Murphy, Olivera Mitrasinovic, and William Ju for valuable assistance with experiments.

Received: December 8, 2003

Revised: April 19, 2004

Accepted: April 22, 2004

Published: May 26, 2004

#### References

- Alvarez-Buylla, A., and Garcia-Verdugo, J.M. (2002). Neurogenesis in adult subventricular zone. *J. Neurosci.* 22, 629–634.
- Alvarez-Buylla, A., Kim, J.R., and Nottebohm, F. (1990). Birth of projection neurons in adult avian brain may be related to perceptual or motor learning. *Science* 249, 1444–1446.
- Alvarez-Buylla, A., Seri, B., and Doetsch, F. (2002). Identification of neural stem cells in the adult vertebrate brain. *Brain Res. Bull.* 57, 751–758.
- Avidsson, A., Kokaia, Z., and Lindvall, O. (2001). N-methyl-D-aspartate receptor-mediated increase of neurogenesis in adult rat dentate gyrus following stroke. *Eur. J. Neurosci.* 14, 10–18.
- Bear, M.F., and Malenka, R.C. (1994). Synaptic plasticity: LTP and LTD. *Curr. Opin. Neurobiol.* 4, 389–399.
- Bjorklund, A., and Lindvall, O. (2000). Cell replacement therapies for central nervous system disorders. *Nat. Neurosci.* 3, 537–544.
- Brown, J., Cooper-Kuhn, C.M., Kempermann, G., Van Praag, H., Winkler, J., Gage, F.H., and Kuhn, H.G. (2003). Enriched environment and physical activity stimulate hippocampal but not olfactory bulb neurogenesis. *Eur. J. Neurosci.* 17, 2042–2046.
- Cai, L., Morrow, E.M., and Cepko, C.L. (2000). Misexpression of basic helix-loop-helix genes in the murine cerebral cortex affects cell fate choices and neuronal survival. *Development* 127, 3021–3030.
- Cameron, H.A., and McKay, R. (1998). Stem cells and neurogenesis in the adult brain. *Curr. Opin. Neurobiol.* 8, 677–680.
- Cameron, H.A., McEwen, B.S., and Gould, E. (1995). Regulation of adult neurogenesis by excitatory input and NMDA receptor activation in the dentate gyrus. *J. Neurosci.* 15, 4687–4692.

- Cau, E., Gradwohl, G., Casarosa, S., Kageyama, R., and Guillemot, F. (2000). *Hes* genes regulate sequential stages of neurogenesis in the olfactory epithelium. *Development* 127, 2323–2332.
- Cau, E., Casarosa, S., and Guillemot, F. (2002). *Mash1* and *Ngn1* control distinct steps of determination and differentiation in the olfactory sensory neuron lineage. *Development* 129, 1871–1880.
- Cecchi, G.A., Petreanu, L.T., Alvarez-Buylla, A., and Magnasco, M.O. (2001). Unsupervised learning and adaptation in a model of adult neurogenesis. *J. Comput. Neurosci.* 11, 175–182.
- Chambers, R.A., Potenza, M.N., Hoffman, R.E., and Miranker, W. (2004). Simulated apoptosis/neurogenesis regulates learning and memory capabilities of adaptive neural networks. *Neuropsychopharmacology* 4, 747–758.
- Claiborne, B.J., Amaral, D.G., and Cowan, W.M. (1990). Quantitative, three-dimensional analysis of granule cell dendrites in the rat dentate gyrus. *J. Comp. Neurol.* 302, 206–219.
- Deisseroth, K., Bito, H., and Tsien, R.W. (1996). Signaling from synapse to nucleus: postsynaptic CREB phosphorylation during multiple forms of hippocampal synaptic plasticity. *Neuron* 16, 89–101.
- Deisseroth, K., Heist, E.K., and Tsien, R.W. (1998). Translocation of calmodulin to the nucleus supports CREB phosphorylation in hippocampal neurons. *Nature* 392, 198–202.
- Deisseroth, K., Mermelstein, P.G., Xia, H., and Tsien, R.W. (2003). Signaling from synapse to nucleus: the logic behind the mechanisms. *Curr. Opin. Neurobiol.* 13, 354–365.
- Feng, R., Rampon, C., Tang, Y.P., Shrom, D., Jin, J., Kyin, M., Sopher, B., Miller, M.W., Ware, C.B., Martin, G.M., et al. (2001). Deficient neurogenesis in forebrain-specific presenilin-1 knockout mice is associated with reduced clearance of hippocampal memory traces. *Neuron* 32, 911–926.
- Filippov, V., Kronenberg, G., Pivneva, T., Reuter, K., Steiner, B., Wang, L.P., Yamaguchi, M., Kettenmann, H., and Kempermann, G. (2003). Subpopulation of nestin-expressing progenitor cells in the adult murine hippocampus shows electrophysiological and morphological characteristics of astrocytes. *Mol. Cell. Neurosci.* 23, 373–382.
- Gardner-Medwin, A.R., and Nicholson, C. (1983). Changes of extracellular potassium activity induced by electric current through brain tissue in the rat. *J. Physiol.* 335, 375–392.
- Gould, E., Tanapat, P., Rydel, T., and Hastings, N. (2000). Regulation of hippocampal neurogenesis in adulthood. *Biol. Psychiatry* 48, 715–720.
- Gould, E., Vail, N., Wagers, M., and Gross, C.G. (2001). Adult-generated hippocampal and neocortical neurons in macaques have a transient existence. *Proc. Natl. Acad. Sci. USA* 98, 10910–10917.
- Graham, B., and Willshaw, D. (1999). Probabilistic synaptic transmission in the associative net. *Neural Comput.* 11, 117–137.
- Hopfield, J.J., and Tank, D.W. (1986). Computing with neural circuits: a model. *Science* 233, 625–633.
- Jan, Y.N., and Jan, L.Y. (1993). HLH proteins, fly neurogenesis, and vertebrate myogenesis. *Cell* 75, 827–830.
- Jefferys, J.G. (1995). Nonsynaptic modulation of neuronal activity in the brain: electric currents and extracellular ions. *Physiol. Rev.* 75, 689–723.
- Jinnah, H.A., Sepkuty, J.P., Ho, T., Yitta, S., Drew, T., Rothstein, J.D., and Hess, E.J. (2000). Calcium channel agonists and dystonia in the mouse. *Mov. Disord.* 15, 542–551.
- Kandel, E.R. (2001). The molecular biology of memory storage: a dialogue between genes and synapses. *Science* 294, 1030–1038.
- Kempermann, G., Gast, D., Kronenberg, G., Yamaguchi, M., and Gage, F.H. (2003). Early determination and long-term persistence of adult-generated new neurons in the hippocampus of mice. *Development* 130, 391–399.
- Kokaia, Z., and Lindvall, O. (2003). Neurogenesis after ischaemic brain insults. *Curr. Opin. Neurobiol.* 13, 127–132.
- Krystal, J.H., D'Souza, D.C., Mathalon, D., Perry, E., Belger, A., and Hoffman, R. (2003). NMDA receptor antagonist effects, cortical glutamatergic function, and schizophrenia: toward a paradigm shift in medication development. *Psychopharmacology (Berl)* 169, 215–233.
- Liu, J., Solway, K., Messing, R.O., and Sharp, F.R. (1998). Increased neurogenesis in the dentate gyrus after transient global ischemia in gerbils. *J. Neurosci.* 18, 7768–7778.
- Louissant, A., Rao, S., Leventhal, C., and Goldman, S.A. (2002). Coordinated interaction of angiogenesis and neurogenesis in the adult songbird brain. *Neuron* 34, 945–960.
- Longo, V.G., Massotti, M., DeMedici, D., and Valerio, A. (1988). Modifications of brain electrical activity after activation of the benzodiazepine receptor types in rats and rabbits. *Pharmacol. Biochem. Behav.* 29, 785–790.
- Madsen, T.M., Treschow, A., Bengzon, J., Bolwig, T.G., Lindvall, O., and Tingstrom, A. (2000). Increased neurogenesis in a model of electroconvulsive therapy. *Biol. Psychiatry* 47, 1043–1049.
- Malberg, J.E., Eisch, A.J., Nestler, E.J., and Duman, R.S. (2000). Chronic antidepressant treatment increases neurogenesis in adult rat hippocampus. *J. Neurosci.* 20, 9104–9110.
- Malenka, R.C., and Nicoll, R.A. (1999). Long-term potentiation—a decade of progress? *Science* 285, 1870–1874.
- Malenka, R.C., Kocsis, J.D., Ransom, B.R., and Waxman, S.G. (1981). Modulation of parallel fiber excitability by postsynaptically mediated changes in extracellular potassium. *Science* 214, 339–341.
- Mao, Z., Bonni, A., Xia, F., Nadal-Vicens, M., and Greenberg, M.E. (1999). Neuronal activity-dependent cell survival mediated by transcription factor MEF2. *Science* 286, 785–790.
- McClelland, J.L., and Rumelhart, D.E. (1985). Distributed memory and the representation of general and specific information. *J. Exp. Psychol. Gen.* 114, 159–197.
- McEwen, B.S. (1994). Corticosteroids and hippocampal plasticity. *Ann. N Y Acad. Sci.* 746, 134–142.
- Mitrasinovic, O.M., Perez, G.V., Zhao, F., Lee, Y.L., Poon, C., and Murphy, G.M., Jr. (2001). Overexpression of macrophage colony-stimulating factor receptor on microglial cells induces an inflammatory response. *J. Biol. Chem.* 276, 30142–30149.
- Monje, M.L., Mizumatsu, S., Fike, J.R., and Palmer, T.D. (2002). Irradiation induces neural precursor-cell dysfunction. *Nat. Med.* 8, 955–962.
- Nacher, J., Crespo, C., and McEwen, B.S. (2001). Doublecortin expression in the adult rat telencephalon. *Eur. J. Neurosci.* 14, 629–644.
- Nakatomi, H., Kuriu, T., Okabe, S., Yamamoto, S., Hatano, O., Kawahara, N., Tamura, A., Kirino, T., and Nakafuku, M. (2002). Regeneration of hippocampal pyramidal neurons after ischemic brain injury by recruitment of endogenous neural progenitors. *Cell* 110, 429–441.
- Nottebohm, F. (2002). Neuronal replacement in adult brain. *Brain Res. Bull.* 57, 737–749.
- Okada, A., Lansford, R., Weimann, J.M., Fraser, S.E., and McConnell, S.K. (1999). Imaging cells in the developing nervous system with retrovirus expressing modified green fluorescent protein. *Exp. Neurol.* 156, 394–406.
- Palmer, T.D., Takahashi, J., and Gage, F.H. (1997). The adult rat hippocampus contains primordial neural stem cells. *Mol. Cell. Neurosci.* 8, 389–404.
- Palmer, T.D., Markakis, E.A., Willhoite, A.R., Safar, F., and Gage, F.H. (1999). Fibroblast growth factor-2 activates a latent neurogenic program in neural stem cells from diverse regions of the adult CNS. *J. Neurosci.* 19, 8487–8497.
- Parent, J.M., Yu, T.W., Leibowitz, R.T., Geschwind, D.H., Sloviter, R.S., and Lowenstein, D.H. (1997). Dentate granule cell neurogenesis is increased by seizures and contributes to aberrant network reorganization in the adult rat hippocampus. *J. Neurosci.* 17, 3727–3738.
- Park, K.I., Teng, Y.D., and Snyder, E.Y. (2002). The injured brain interacts reciprocally with neural stem cells supported by scaffolds to reconstitute lost tissue. *Nat. Biotechnol.* 20, 1111–1117.
- Petreanu, L., and Alvarez-Buylla, A. (2002). Maturation and death of adult-born olfactory bulb granule neurons: role of olfaction. *J. Neurosci.* 22, 6106–6113.
- Rochefort, C., Gheusi, G., Vincent, J.D., and Lledo, P.M. (2002). Enriched odor exposure increases the number of newborn neurons in the adult olfactory bulb and improves odor memory. *J. Neurosci.* 22, 2679–2689.

- Sah, P., Hestrin, S., and Nicoll, R.A. (1989). Tonic activation of NMDA receptors by ambient glutamate enhances excitability of neurons. *Science* 246, 815–818.
- Santarelli, L., Saxe, M., Gross, C., Surget, A., Battaglia, F., Dulawa, S., Weisstaub, N., Lee, J., Duman, R., Arancio, O., et al. (2003). Requirement of hippocampal neurogenesis for the behavioral effects of antidepressants. *Science* 301, 805–809.
- Schwab, M.H., Bartholomae, A., Heimrich, B., Feldmeyer, D., Druffel-Augustin, S., Goebbels, S., Naya, F.J., Zhao, S., Frotscher, M., Tsai, M.J., and Nave, K.A. (2000). Neuronal basic helix-loop-helix proteins (NEX and BETA2/Neuro D) regulate terminal granule cell differentiation in the hippocampus. *J. Neurosci.* 20, 3714–3724.
- Seaberg, R.M., and van der Kooy, D. (2002). Adult rodent neurogenic regions: the ventricular subependyma contains neural stem cells, but the dentate gyrus contains restricted progenitors. *J. Neurosci.* 22, 1784–1793.
- Seri, B., Garcia-Verdugo, J.M., McEwen, B.S., and Alvarez-Buylla, A. (2001). Astrocytes give rise to new neurons in the adult mammalian hippocampus. *J. Neurosci.* 18, 7153–7160.
- See, V., Boutillier, A.L., Bito, H., and Loeffler, J.P. (2001). Calcium/calmodulin-dependent protein kinase type IV (CaMKIV) inhibits apoptosis induced by potassium deprivation in cerebellar granule neurons. *FASEB J.* 15, 134–144.
- Sejnowski, T.J. (1999). The book of Hebb. *Neuron* 24, 773–776.
- Shihabuddin, L.S., Horner, P.J., Ray, J., and Gage, F.H. (2000). Adult spinal cord stem cells generate neurons after transplantation in the adult dentate gyrus. *J. Neurosci.* 20, 8727–8735.
- Shors, T.J., Miesegaes, G., Beylin, A., Zhao, M., Rydel, T., and Gould, E. (2001). Neurogenesis in the adult is involved in the formation of trace memories. *Nature* 410, 372–376.
- Snyder, E.Y., Yoon, C., Flax, J.D., and Macklis, J.D. (1997). Multipotent neural precursors can differentiate toward replacement of neurons undergoing targeted apoptotic degeneration in adult mouse neocortex. *Proc. Natl. Acad. Sci. USA* 94, 11663–11668.
- Song, H., Stevens, C.F., and Gage, F.H. (2002). Astroglia induce neurogenesis from adult neural stem cells. *Nature* 417, 39–44.
- Squire, L.R., and Zola-Morgan, S. (1991). The medial temporal lobe memory system. *Science* 253, 1380–1386.
- Suhonen, J.O., Peterson, D.A., Ray, J., and Gage, F.H. (1996). Differentiation of adult hippocampus-derived progenitors into olfactory neurons in vivo. *Nature* 383, 624–627.
- Tanigaki, K., Nogaki, F., Takahashi, J., Tashiro, K., Kurooka, H., and Honjo, T. (2001). Notch1 and Notch3 instructively restrict bFGF-responsive multipotent neural progenitor cells to an astroglial fate. *Neuron* 29, 45–55.
- Taupin, P., and Gage, F.H. (2002). Adult neurogenesis and neural stem cells of the central nervous system in mammals. *J. Neurosci. Res.* 69, 745–749.
- Temple, S. (2001). The development of neural stem cells. *Nature* 414, 112–117.
- Toma, J.G., El-Bizri, H., Barnabe-Heider, F., Aloyz, R., and Miller, F.D. (2000). Evidence that helix-loop-helix proteins collaborate with retinoblastoma tumor suppressor protein to regulate cortical neurogenesis. *J. Neurosci.* 20, 7648–7656.
- Tsien, R.W., Lipscombe, D., Madison, D., Bley, K., and Fox, A. (1995). Reflections on Ca(2+)-channel diversity, 1988–1994. *Trends Neurosci.* 18, 52–54.
- van Praag, H., Christie, B.R., Sejnowski, T.J., and Gage, F.H. (1999). Running enhances neurogenesis, learning, and long-term potentiation in mice. *Proc. Natl. Acad. Sci. USA* 96, 13427–13431.
- Wang, S., Sdrulla, A., Johnson, J.E., Yokota, Y., and Barres, B.A. (2001). A role for the helix-loop-helix protein Id2 in the control of oligodendrocyte development. *Neuron* 29, 603–614.
- Wang, D.D., Krueger, D.D., and Bordey, A. (2003). Biophysical properties and ionic signature of neuronal progenitors of the postnatal subventricular zone in situ. *J. Neurophysiol.* 90, 2291–2302.
- Watt, F.M., and Hogan, B.L. (2000). Out of Eden: stem cells and their niches. *Science* 287, 1427–1430.
- West, A.E., Chen, W.G., Dalva, M.B., Dolmetsch, R.E., Kornhauser, J.M., Shaywitz, A.J., Takasu, M.A., Tao, X., and Greenberg, M.E. (2001). Calcium regulation of neuronal gene expression. *Proc. Natl. Acad. Sci. USA* 98, 11024–11031.
- Westerlund, U., Moe, M.C., Varghese, M., Berg-Johnsen, J., Ohlsson, M., Langmoen, I.A., and Svensson, M. (2003). Stem cells from the adult human brain develop into functional neurons in culture. *Exp. Cell Res.* 289, 378–383.
- Wheeler, D.B., Randall, A., and Tsien, R.W. (1994). Roles of N-type and Q-type Ca<sup>2+</sup> channels in supporting hippocampal synaptic transmission. *Science* 264, 107–111.
- Willshaw, D.J., Buneman, O.P., and Longuet-Higgins, H.C. (1969). Non-holographic associative memory. *Nature* 222, 960–962.